LOAD-INJECTED DC CURRENT IN DISTRIBUTION TRANSFORMERS

Ayesha Iroshani Herath

139561T

Degree of Master of Science in Electrical Installation

Department of Electrical Engineering

University of Moratuwa

Sri Lanka

June 2017

LOAD-INJECTED DC CURRENT IN DISTRIBUTION TRANSFORMERS

Herath Mudiyanselage Ayesha Iroshani Herath

139561T

Dissertation submitted in partial fulfillment of the requirements for the degree Master of Science in Electrical Installation

Department of Electrical Engineering

University of Moratuwa

Sri Lanka

June 2017

DECLARATION

I declare that this is my own work and this dissertation does not incorporate without acknowledgement any material previously submitted for a Degree or Diploma in any other University or institute of higher learning and to the best of my knowledge and belief it does not contain any material previously published or written by another person except where the acknowledgement is made in the text.

Also, I hereby grant to University of Moratuwa the non-exclusive right to reproduce and distribute my dissertation, in whole or in part in print, electronic or other medium. I retain the right to use this content in whole or part in future works (such as articles or books).

Signature: Date:

The above candidate has carried out research for the Masters Dissertation under my supervision.

Signature of the Supervisor: Date:

ABSTRACT

Power electronic based loads and other non-linear loads on the utility system create small amounts of DC current on top of their normal AC current. Due to heavy proliferation of such loads on the present day utility system, the net DC current accumulated at the secondary of the distribution transformer is significant. This DC-current offsets the operating point of the magnetization characteristic for the iron core, and creates a severe asymmetry between the positive and negative half cycles of the magnetization current, both in magnitude and shape, owing to magnetic saturation. It directly affects the shape of input current, and also recreates a DC current at input with magnitude even higher than that present at the secondary.

This project is about investigating the effects on primary (supply) current due to DC current in the secondary of a transformer, and eliminating such effects altogether by diverting DC current away from the secondary with a suitable power electronic controller.

Investigations were carried out by simulations, after developing a model for the magnetization characteristic for the transformer, based on test data. Simulations were carried out in MATLAB for different combinations of AC and DC current in the secondary, and the results obtained were compared and discussed against the experimental observations made on the real transformer.

DC current diversion away from the transformer secondary was done by measuring the load-demanded (or returned) DC current, and injecting (or absorbing) an equal DC current at the secondary terminals. This was a complex task because measuring a small DC current superimposed with a large AC current was not straightforward, and also injecting a small DC current accurately against a large AC voltage present across the transformer secondary was not straightforward. However, both these challenges were successfully overcome and an extremely good DC current diversion system developed. All details of the design are given and described in the report.

ACKNOWLEDGEMENT

This page is dedicated to convey my gratitude for those who were with me helping, encouraging and enriching my knowledge and also others who helped me in various ways. Therefore I take this opportunity to offer the thanks of honor to every person who gave me their guidance and assistance to achieve this goal.

First of all I would like to convey my heartiest gratefulness to my supervisor, Prof. J.P. Karunadasa for giving me warm welcome in knowledge-seeking quest, and guiding and assisting me by dedicating his valuable time.

Next, I would like to convey my warm appreciation to the Head of the Department of Electrical Engineering, Prof. N.K.Wickramarachchi, for allowing me to use the equipment and facilities in the Department, and to the Coordinator of the Electrical Installation Course, Dr.W.D.Prasad, for his admirable assistance.

Also, I would like to extend my sincere gratitude to the staff of the Electrical Machines Laboratory in the university for providing support to conduct laboratory experiments successfully.

Further, I wish to thank all members of the academic and non-academic staff of the Department of Electrical Engineering for helping me in numerous other ways to make my research a success

My special thank goes to the staff of the Arthur C Clark Institute of Modern Technology for giving permission and assistance for collecting practical data related to the project

Finally, I wish to accord my heartfelt gratitude to my parents, relatives and colleagues who supported and encouraged me in many ways throughout the project.

TABLE OF CONTENTS

LIST OF FIGURES

LIST OF TABLES

LIST OF APPENDICES

CHAPTER 1

INTRODUCTION

The proliferation of nonlinear loads and power electronic driven loads on the power distribution system (mostly ac & dc drives, computers and grid-tie inverters) introduce power quality problems in the distribution network, such as harmonic distortions, voltage notches, voltage spikes, voltage unbalances, voltage sags, voltage swells etc. A significant cause among these effects is injection of DC current back to the distribution network by the loads. DC current injected by individual loads add up to some significant level at the point of common coupling (PCC) and it directly influences the operation of the distribution transformer and associated other components and systems. Grid connected inverters, such as solar power inverters introduce a noticeable component of DC current in to the system.

A DC current component is particularly detrimental to the distribution power transformers, because it can lead to asymmetric magnetic core saturation. Transformer cores have very high magnetic conductivity, so even small DC current can excite the transformer to have large effects. Transformers operating under saturation conditions present distortion in magnetizing and hence supply current, increased power losses, overheating and reduced lifespan etc. Other specific problems created by DC current in an AC power network are corrosion in underground equipment, errors in metering, malfunctioning of protective equipment, overheating of other grid connected equipment such as capacitor banks and AC machines etc. [1, 2, 3, 4].

1.1 Problem Statement

Some loads connected to distribution network return small DC current components back to the network which add to significant total at the transformer to saturate its core. This can create significant operational issues to the transformer itself and the system upstream. This DC current component and the corresponding DC voltage component can induce metering errors and malfunction of protection system, leading to adverse effect on the distribution network.

1.2 Objectives of the study

Objectives of the study are:

1. To investigate effects of DC current (injected by loads) on the operation of distribution transformers
2. To design and test a system to eliminate DC current from circulating through the secondary of a distribution transformer

1.3 Research Methodology

The following steps are taken to achieve the final outcome.

(i). Reviewing published literature on load-injected DC current in distribution systems
(ii). Gathering data in a real distribution system on superimposed DC current
(iii). Investigating in laboratory the effects of load-injected DC current on the operation of a transformer
(iv). Developing a self-tuned simulation model for a transformer capable of accommodating magnetic saturation caused by DC current
(v). Simulating performance of a transformer for different injected DC conditions
(vi). Designing DC current sensor
(vii). Designing DC current elimination (converter) system with closed loop control
(viii). Testing and validating the complete system in MATLAB environment
(ix). Drawing out conclusions and recommendations

CHAPTER 2

LITERATURE REVIEW

At the moment this problem of load-injected DC current in transformers is addressed by international or country-specific regulations that impose limits on the maximum DC current injected by influential loads in to the grid. For example, Table 1 gives the existing guidelines and regulations in five selected countries for grid-tie inverters.

Table 1.1: Limits of DC current injection permitted by different countries for grid-tie inverters (LV system)

Country	**Standard**	**Maximum permitted DC current**
United Kingdom	ER G83/1	0.25 % of rated current of the inverter
Australia	AS 4777.2	0.5% of rated current of the inverter or 5mA , whichever greater
USA	IEEE 929-2000 IEEE 1547	0.5% of rated current of the inverter 0.5% of rated current of the inverter
Switzerland	IEC 61727	1% of rated current of the inverter
Germany	DINVDE 0126-1-1	1A (Total injection) [States in the case of DC current injection greater than 1A, disconnection is mandatory in 0.2S]

A significant attention has been given in the literature for limiting DC current injected by grid-tie inverters due to its relative significance. Three methods have been proposed for connecting inverters with the utility system [5, 6], namely the Line frequency transformer interconnection, transformerless interconnection and high frequency transformer interconnection. Each has its own advantages and disadvantages.

1. Line frequency transformer interconnection

   Line frequency transformer is employed between inverter and the grid to eliminate DC current injected in to the grid (see Figure 2.1). This transformer is large, heavy and forms a substantial cost in the grid connected system and it contributes to significant power losses, lowering inverter efficiency by about 1–2% [3, 7].

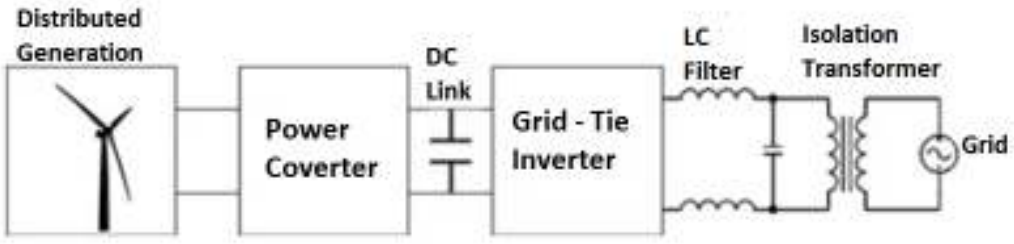

Figure 2.1: Grid-tie inverter configuration using line frequency transformer [3]

2. Transformerless interconnection

(i). Blocking DC current with an AC capacitor

Transformerless interconnection proposes a DC blocking capacitor in the inverter output (see Figure 2.2). However, this might be impractical due to the voltage drop across the AC capacitor, which is in series. To have minimum voltage drop across the capacitor, it requires a large and expensive AC capacitor of low reactance at 50Hz line frequency [3].

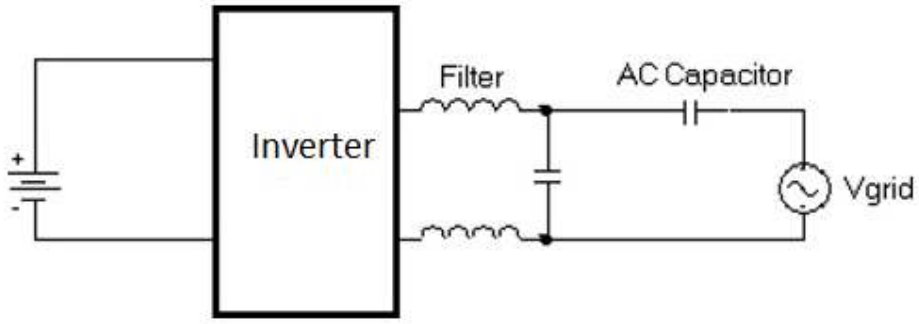

Figure 2.2: Blocking DC current with an AC capacitor [3]

(ii). Half-bridge inverter

An alternative transformerless interconnection uses a half bridge inverter at the inverter output (see Figure 2.3),which is inherently blocking DC current because at least one of the capacitors is always present in the output conduction path and hence there can be no DC current flow into the grid.

But this topology requires a DC link voltage twice the inverter output voltage, and correspondingly higher rating of inverter components, adding to higher cost and reduced system efficiency [3, 5].

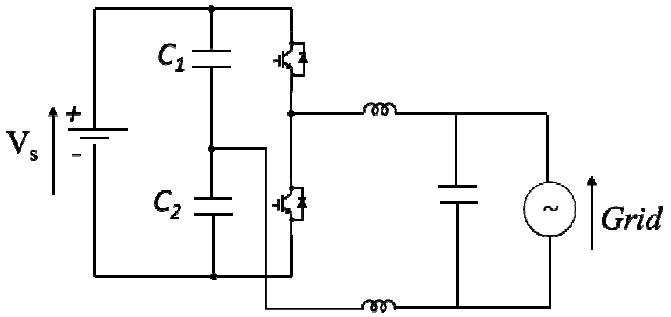

Figure 2.3: Half bridge inverter [3, 5]

(iii). DC offset sensor with current controller

Another transformerless interconnection (Figure 2.4) proposes a DC offset sensor (Figure 2.5) and current controller (Figure 2.6), which too adds to drawback of larger size, high cost and losses to the system [8]. In this arrangement, DC component in the inverter output is reduced by the current controller. DC offset sensor provides the information of DC voltage present in the inverter output and hence a negative DC offset demand is made at the current controller to reduce DC current injected to the grid.

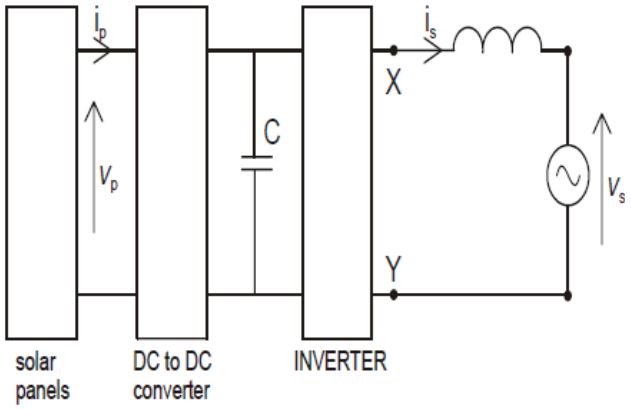

Figure 2.4: Transformerless interconnection [4]

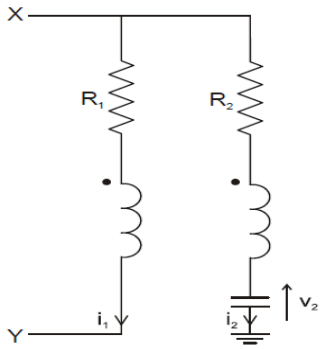

Figure 2.5: DC offset sensor [4]

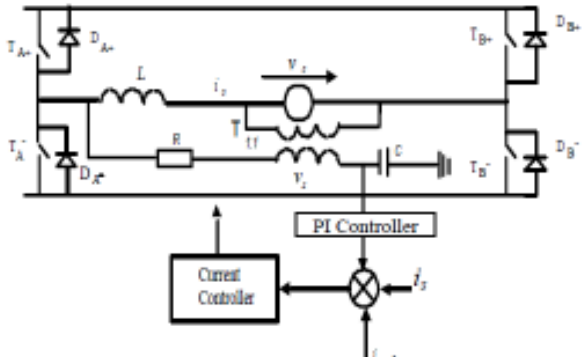

Figure 2.6: DC offset controller [9]

3. High frequency transformer interconnection

High frequency transformer interconnection (Figure 2.7) does not guarantee DC component cancellation and has reduced efficiency/cost ratio due to several stages [10].

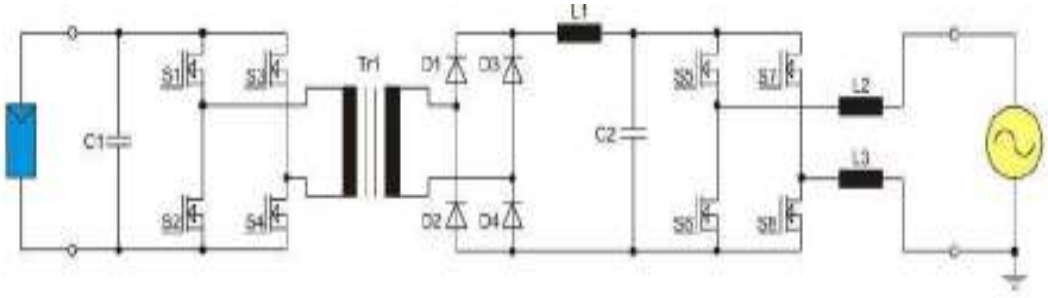

Figure 2.7: HF Transformer Interconnection [11]

Although actions are taken to limit the contribution of DC current from individual loads the net summation of DC current at the secondary of a transformer can still be significant. This is because the number of loads connected to the transformer is high. Therefore, a summative means is required to address the problem of DC magnetization of the transformer. The methods of blocking DC current in grid-tie inverters are good starting points for the investigation of a suitable strategy to develop a system to divert DC current away from the secondary winding of the distribution transformer.

CHAPTER 3

PRACTICAL INVESTIGATION OF THE EFFECTS OF DC CURRENT IN THE OPERATION OF A TRANSFORMER

3.1 DC Current in a Sample Distribution System

To study the significance of DC current in a real system, a sample power distribution system of the Arthur C Clark Institution of Modern Technologies was chosen. This system is fed by an 11kV/400V, 400kVA, 50Hz three phase step down transformer and the loads comprised a significant count of personal computers and electronic equipment among other loads. Measurements were carried out using FLUKE 435 Power Quality Analyser at the transformer secondary, which is the PCC for the particular power system (see Figure 3.1). Screen-shot of Figure 3.2 gives the values of different measurement of the load, and Figure 3.3 gives the spectrum of currents for three phases. It is observed that the net DC current at the PCC of three phases are 1.1 A, 1.5 A and 1.4 A, all of which are well above the upper limit given in the standards in Table 1.

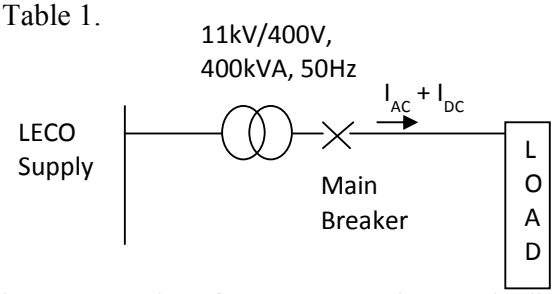

Figure 3.1: Point of measurement in sample distribution system

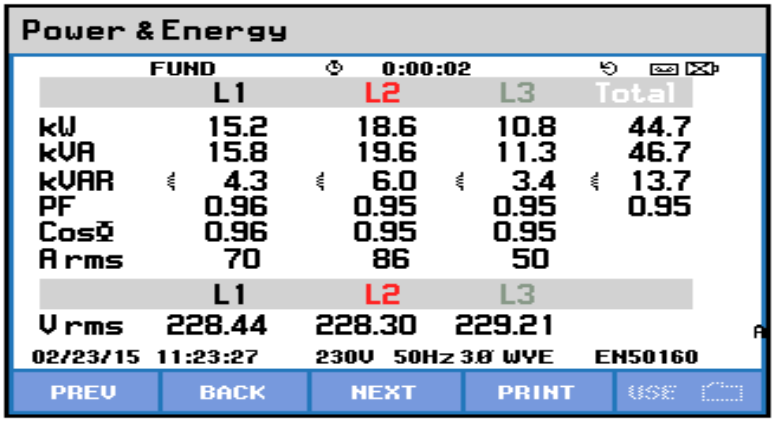

Figure 3.2: Power and Energy data in the sample distribution system

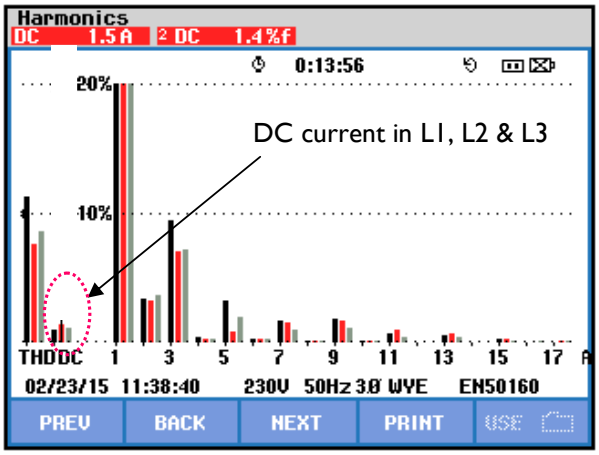

Figure 3.3: DC current measurement in phase 1, 2 and 3

3.2 Laboratory Investigation of the Effect of DC Current in a Transformer

To study the effects of DC current on the operation of a transformer, a 4 kVA, 230/400 V single phase laboratory transformer was selected, in the first place.

Transformer primary rating = 230V, 17.4 A

Transformer secondary rating = 400V, 10 A

Transformer was subjected to four tests to ensure its normal operation and effects of DC current injection.

Test 1 - Magnetizing current at rated voltage

Test 2 - Primary current on load

Test 3 - Primary current on load with heavy DC current injected at the secondary

Test 4 -Primary current on load with a small DC current injected at the secondary

3.2.1 Magnetizing current at rated voltage

To measure magnetizing current at rated voltage, the transformer secondary side was kept open and 230 V (rated voltage) applied to the primary side. Figure 3.4 shows the test schematic for this test.

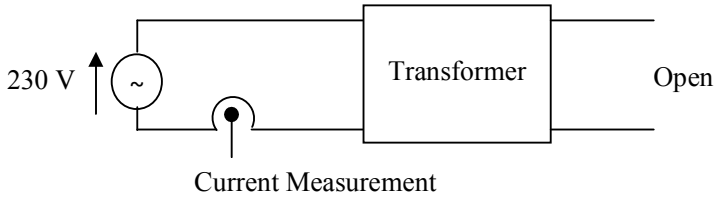

Figure 3.4: Test schematic for the test 1

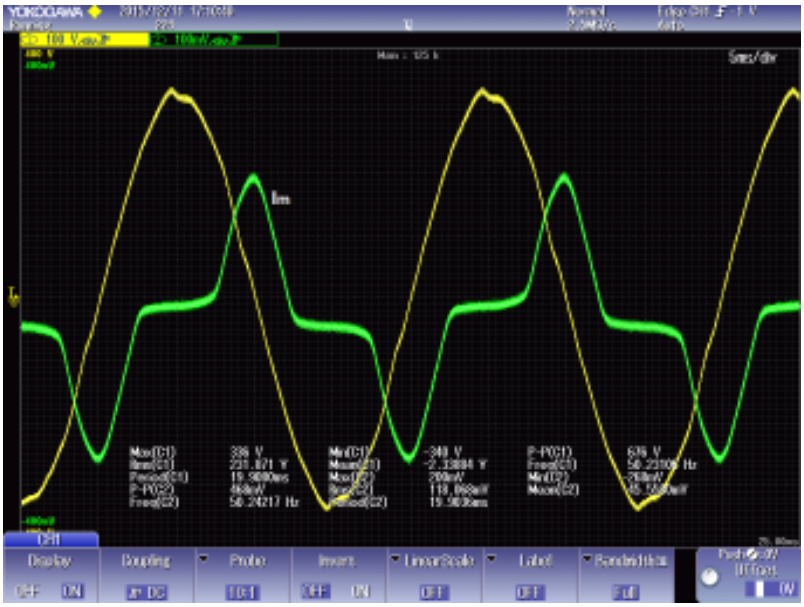

Figure 3.5: Tested magnetizing current (I_m) at rated input voltage

Magnetizing current measured at rated voltage on LV side is given in Figure 3.5 which complies with theoretical expectations, having a significant 3rd harmonic component. This is an obvious consequence of the inherent magnetic saturation of the core but the positive and negative half cycles (2.6 A peak) are similar implying symmetrical magnetization.

3.2.2 Primary current on load

To measure primary current on load, a 45Ω resistive load (corresponding to 90% full load) was connected to the secondary and 230V (rated voltage) applied to the primary, as shown in Figure 3.6.

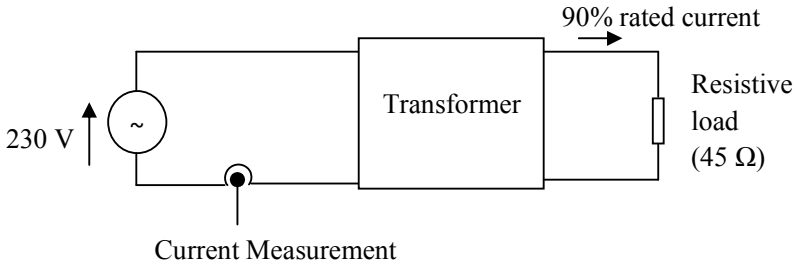

Figure 3.6: Test schematic for the test 2

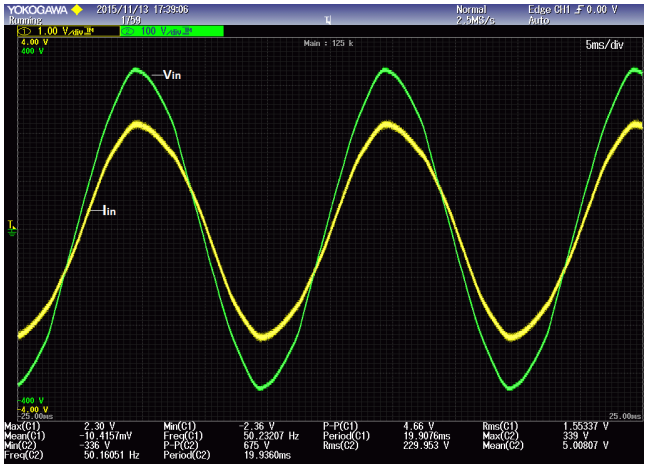

Figure 3.7: Primary current (I_{in}) & voltage (V_{in}) waveforms on load

The net primary current of the transformer should be almost sinusoidal because it is dominated by the sinusoidal load current. The magnetizing current is only a small fraction of the total current and hence the distortions present in magnetizing current are not visible in the net primary current. The tested primary current and voltage are shown in Figure 3.7. It can be observed that the current waveform is now sinusoidal, and inphase with the voltage (23 A peak).

3.3.3 Primary current on load with heavy DC current injected to the secondary

To investigate the effects of heavy DC current on the operation of the transformer, a DC current component amounting to 40% full load current was created by connecting a diode in series with a 45Ω resistive load (corresponding to 90% full load current in its own) at the secondary, as shown in Figure 3.8. This type of heavy DC current is unlikely to occur in practice but consciously chosen for the test to magnify the effects. Primary current waveform (together with voltage waveform) under this condition is given in Figure 3.9 and it clearly shows excessive distortions inflicted on the waveform.

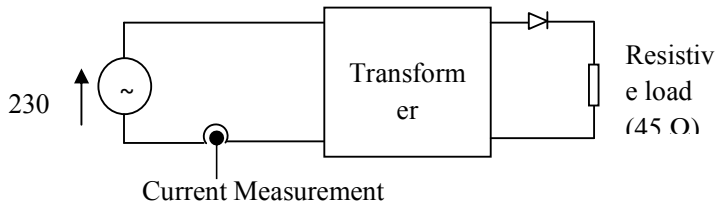

Figure 3.8: Test schematic for the test 3

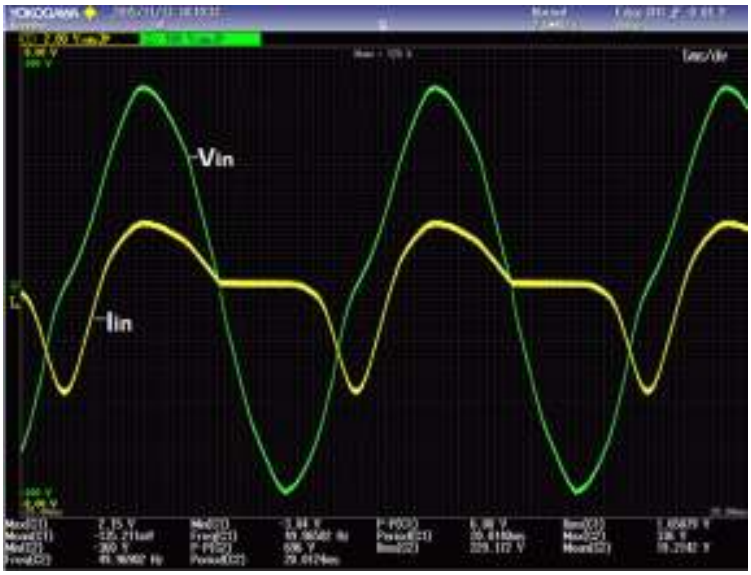

Figure 3.9: Tested primary current and voltage with 40% DC current in the secondary, created by rectification of 90% full load (resistive) current at rated input voltage

The negative peak of the primary current waveform in Figure 3.9 now occurs just about 90° ahead of the positive peak and this is purely a magnetizing current peak. Its value has now reached staggering 38.4 A from its nominal value of 2.6 A in Figure 3.5. The positive peak is almost unchanged (21.5A) which is determined purely by the load. This behavior is in complete agreement with the theoretical predictions.

The DC current injected at the secondary lowers the operating point of the iron core in the flux current characteristic, pushing the negative half cycle of flux deep in to saturating region resulting in a large negative peak of magnetizing current. The amplitude of this negative peak of magnetizing current is well above the negative peak of the load related input current. Thus the negative peak of the resultant primary current occurs right at the location of the same of the magnetizing current, which is 90° behind the negative peak of the voltage. The positive peak of the magnetizing current does not change much as the positive half of the flux waveform is now virtually inside the linear portion of the characteristic, and remains near 2.6 A. Therefore, the resultant primary current waveform retains its positive peak at the same location of the load related current, which is coinciding with the positive peak

of voltage, with almost the same value of 21.5 A. Thus, the phase angle shift between the negative and positive halves of the resultant input current waveform becomes nearly 90°. DC current injection for this test was done by way of connecting a diode in series with the load in the secondary. This is the reason for not having the part of input current waveform in phase with the negative half cycle of voltage.

Input voltage waveform is also now showing some distortions, especially a dip in the value near the positive going zero crossing of the waveform. This is mainly due to the voltage drop in the supply side impedance. This introduces asymmetry to the waveform and thereby a notable 2nd harmonic component.

3.3.4 Primary current on load with a small value of DC current injected at the secondary

To investigate the effects of smaller values of DC current on the operation of the transformer a DC current amounting to 10% of rated current was created in the secondary while the secondary is delivering 90% rated current to a resistive load. This time the DC current was injected with the negative polarity to cause an opposite shifting of the magnetic operating point and saturation in the positive half cycle. Test schematic is given in Figure 3.10.

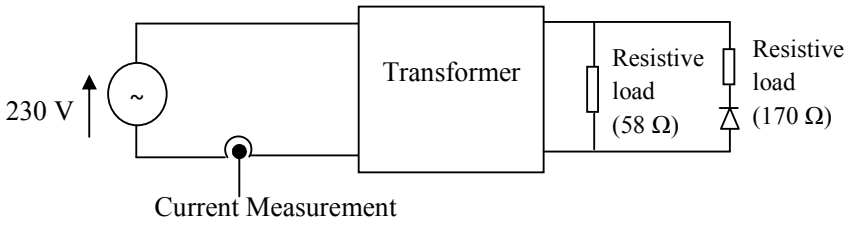

Figure 3.10: Test schematic for the test 4

The resulting primary current and voltage waveforms are given in Figure 3.11. The positive half cycle of current is now "broadened" beyond the zero-crossing of the voltage but the negative half cycle remains relatively unchanged. This behaviour of current is again due to the asymmetry of the magnetizing current, caused by the injected DC current. Now the magnetic operating point is shifted up on the flux-current characteristic and hence the positive half cycle of flux is driven in to hard

saturation, resulting in a very high positive peak of magnetizing current. Although the DC current injected was only 10% rated current, the saturation has raised the positive peak of the magnetizing current from its nominal value of 2.6 A (see Fig.3.5) to about 18 A, as seen in the current waveform at the point 90° behind of the voltage peak. The summation of large positive peak of magnetizing current and the positive peak of load current, which is inphase with the voltage, results in a broader positive half cycle of the primary current. The negative half cycle of primary current remains as of the load related current because the negative peak of the magnetizing current is only below 2.6 A, which is too small compared to the load related current peak of 23 A. The resulting asymmetry between positive and negative half cycles of the primary current gives rise to a net DC current in the input side too.

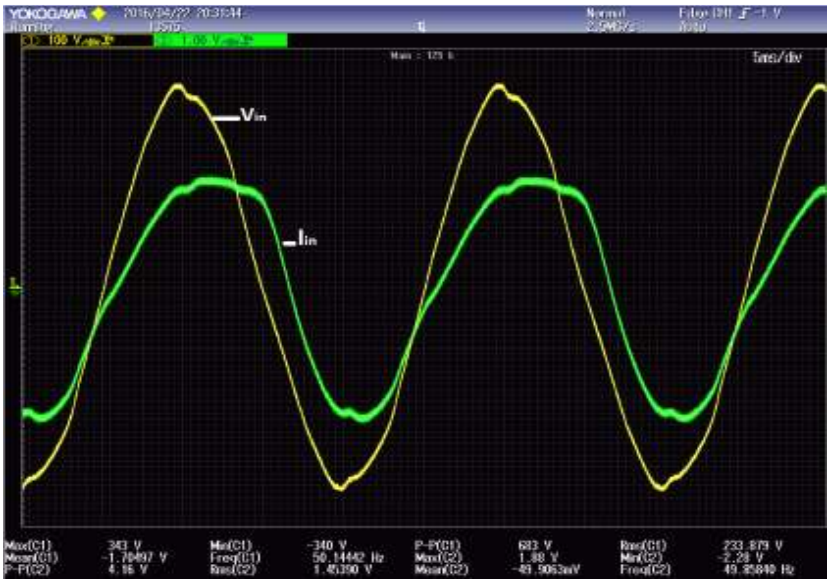

Figure 3.11: Tested primary current and voltage with 10% DC current at 90% load (resistive) at rated input voltage

Results of the experimental investigations reveal the relative significance of the influence of load-injected DC current on the operation of a transformer. They provide justifications on the need for an effective strategy to divert DC current away from the secondary side of the distribution transformers in a utility system.

CHAPTER 4

SIMULATION OF THE EFFECTS OF DC CURRENT IN A TRANSFORMER

4.1 Transformer Model

Practical investigations carried out and described in section 3.2 represent only few handpicked cases. A good simulation model is required for a comprehensive investigation of the effects of DC current on the operation of the transformer, under different operating conditions. Therefore, a MATLAB simulation model corresponding to the equivalent circuit shown in Figure 4.1 was developed for the chosen, 4 kVA, 230 V/400 V, single phase laboratory-transformer.

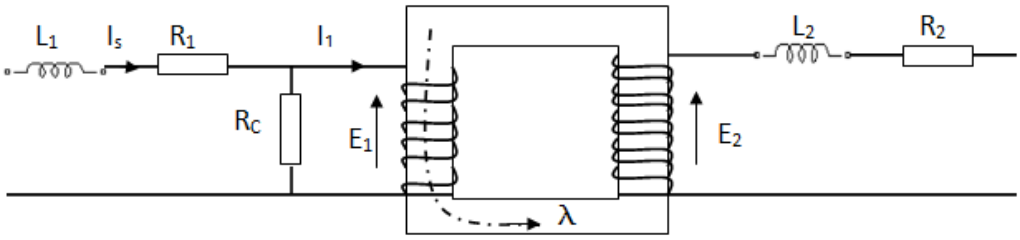

Figure 4.1: Transformer model

λ – flux linkage.
V_s – Input ac voltage
I_s – Input ac current
I_1 – Magnetizing component of input current
E_1 – Induced voltage in the primary winding
E_2 – Induced voltage in the secondary winding
L_1 – Leakage inductance of the primary winding
R_1 – Resistance of the primary winding
L_2 – Leakage inductance of the secondary winding
R_2 – Resistance of the secondary winding
R_c – Resistance of the magnetizing branch (Core loss component)

4.1.1. Deriving parameters for the model

Values for the parameters of the model were estimated by conducting open circuit test and short circuit test on the transformer, whose results are given in Table 3.1.

Table 3.1: Open circuit and short circuit test results

Test	Voltage (V)	Current (A)	Power input (W)
Open circuit test (conducted on 230V side)	230	1.125	40
Short circuit test (conducted on 400V side)	10	10	50

From the open circuit test data,

$$R_c = \frac{V_{oc}^2}{P_{oc}} = \frac{230^2}{40} = 1322.5\ \Omega$$

From the short circuit test data, taking R_{eq} as net resistance referred to 400 V side,

$$R_{eq} = \frac{P_{sc}}{I_{sc}^2} = \frac{50}{10^2} = 0.5\ \Omega \equiv \frac{0.5 * 4000}{400^2}\text{pu} = 0.0125\ \text{pu}$$

Assuming equal per unit resistances in the primary and the secondary windings,

$$R_1 = R_2 = \frac{R_{eq}}{2} = 0.00625\ \text{pu}$$

Therefore,

$$R_1 = \frac{0.00625 * 230^2}{4000} = 0.083\ \Omega$$
$$R_2 = \frac{0.00625 * 400^2}{4000} = 0.025\ \Omega$$

From the short circuit test data, taking X_{eq} as net reactance referred to 400 V side,

$$X_{eq} = \frac{\sqrt{(VI)_{sc}^2 - {P_{sc}}^2}}{I_{sc}^2}$$
$$= \frac{\sqrt{((10 * 10)^2 - 50^2)}}{10^2} = 0.87\ \Omega \equiv \frac{0.87 * 4000}{400^2}\text{pu} = 0.0217\ \text{pu}$$

Assuming equal per unit reactance in the primary and the secondary windings,

$$X_1 = X_2 = \frac{X_{eq}}{2} = 0.0109\ \text{pu}$$

Therefore,

$$X_1 = \frac{0.0109 * 230^2}{4000} = 0.144\ \Omega$$

$$X_2 = \frac{0.0109 * 400^2}{4000} = 0.436\ \Omega$$

Thus,

$$L_1 = \frac{0.144}{2\pi * 50} \equiv 0.458\ \text{mH}$$

$$L_2 = \frac{0.436}{2\pi * 50} \equiv 1.38\ \text{mH}$$

So, the final values of the parameters of the transformer model are:

$L_1 = 0.458$ mH
$L_2 = 1.38$ mH
$R_1 = 0.083\ \Omega$
$R_2 = 0.25\ \Omega$
$R_c = 1322.5\ \Omega$

4.1.2 Deriving magnetization characteristic for the core

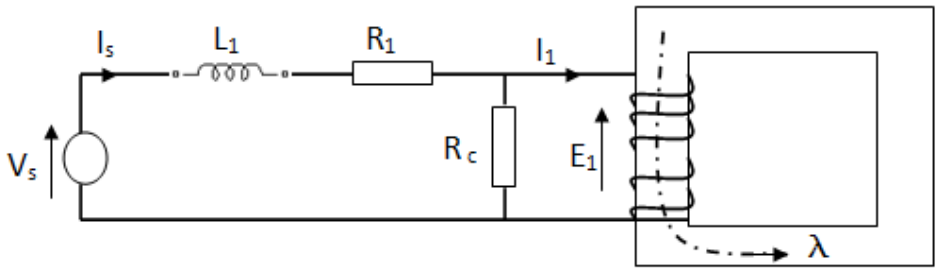

Figure 4.2: No load model

Magnetization characteristic was extracted from the no-load test data, with reference to no-load model given in Figure 4.2. Corresponding mathematical relationships for the transformer are,

$$E_1 = V_s - R_1 I_s - L_1 \frac{dI_s}{dt} \quad [4.1]$$

$$I_1 = I_s - \frac{E_1}{R_c} \quad [4.2]$$

$$\frac{d\lambda}{dt} = E_1 \quad [4.3]$$

Iteration equations to compute relationship between λ and I_1, derived from 4.1, 4.2 and 4.3 are,

$$E_1(k) = V_s(k) - R_1 I_s(k) - \left(\frac{L_1\big(I_s(k+1) - I_s(k)\big)}{\delta t}\right) \quad [4.4]$$

$$I_1(k) = I_s(k) - \frac{E_1(k)}{R_c} \quad [4.5]$$

$$\lambda(k+1) = \lambda(k) + E_1(k)\,\delta t \quad [4.6]$$

R_1, L_1, and R_c are data, and $V_s\,(k)$ and $I_s\,(k)$ are taken from no-load test waveforms. Time step δt is chosen to be smaller as 0.0005s to ensure better accuracy and numerical stability. Figure 4.3 shows the Excel plot of $I_1\,(k)$ versus $\lambda\,(k)$.

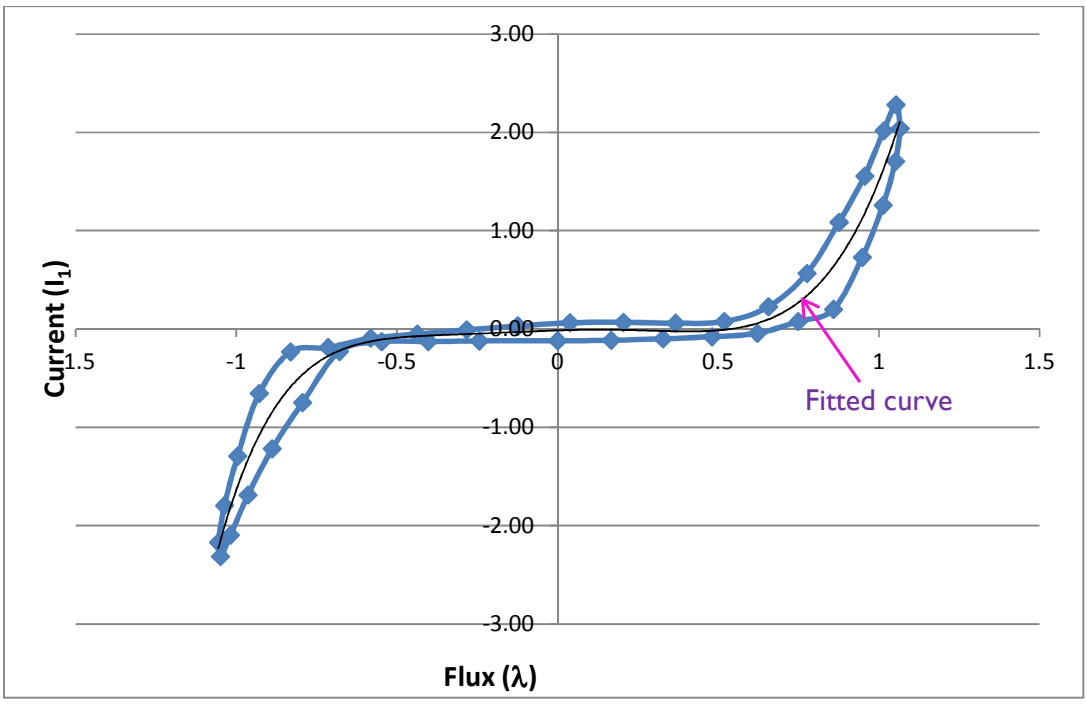

Figure 4.3: Magnetization characteristic for the transformer core

Curve fitting in Excel gave the following mathematical expression for the magnetization characteristic, as a 6th order polynomial.

$$I_1 = -0.4746\lambda^6 + 2.0944\lambda^5 + 0.7191\lambda^4 - 0.6226\lambda^3 - 0.2973\lambda^2 + 0.0999\lambda - 0.014$$

4.2 Simulation of magnetizing current at rated voltage

Primary current under open circuit conditions is modeled by the following equations, with reference to the equivalent circuit in Figure 4.2.

$$L_s \frac{dI_s}{dt} = \left(V_s - r_1 I_s - R_c(I_s - I_1)\right) \quad [4.7]$$

$$\frac{d\lambda}{dt} = R_c(I_s - I_1) \quad [4.8]$$

$$I_1 = -0.4746\lambda^6 + 2.0944\lambda^5 + 0.7191\lambda^4 - 0.6226\lambda^3 - 0.2973\lambda^2 + 0.0999\lambda - 0.014 \quad [4.9]$$

Here, V_s is input voltage and L_s, r_1, R_c are data. Corresponding iteration equations are as follows.

$$V_s(k) = V_m \cos(k\omega\delta t) \quad [4.10]$$

$$I_1(k) = -0.4746\lambda^6(k) + 2.0944\lambda^5(k) + 0.7191\lambda^4(k) - 0.6226\lambda^3(k) - 0.2973\lambda^2(k) + 0.0999\lambda(k) - 0.014 \quad [4.11]$$

$$I_s(k+1) = I_s(k)\left(1 - \frac{\delta t\,(r_1 + R_c)}{L_1}\right) + \frac{\delta t\, V_s(k)}{L_1} + \frac{\delta t\, R_c I_1(k)}{L_1} \quad [4.12]$$

$$\lambda(k+1) = \lambda(k) + \delta t\, R_c\left(I_s(k) - I_1(k)\right) \quad [4.13]$$

Where,

$V_m = 340$ V
$I_1(0) = 0$
$\lambda(0) = 0$, because V_s is selected as a cosωt function
$\delta t = 0.1$ µs

Iteration equations in 4.10 to 4.13 were simulated in Matlab, and the program code is given in the Appendix (Table A.1). The waveform of simulated primary current (I_s) is shown in Figure 4.4, corresponding to rated input voltage of 230 V. Figure 4.5 shows the waveforms of both the simulated primary current and the tested primary current (given in Figure 3.5) for comparisons and two indicate a very close match.

This is a clear evidence of the validity of the model with regard to magnetic saturation.

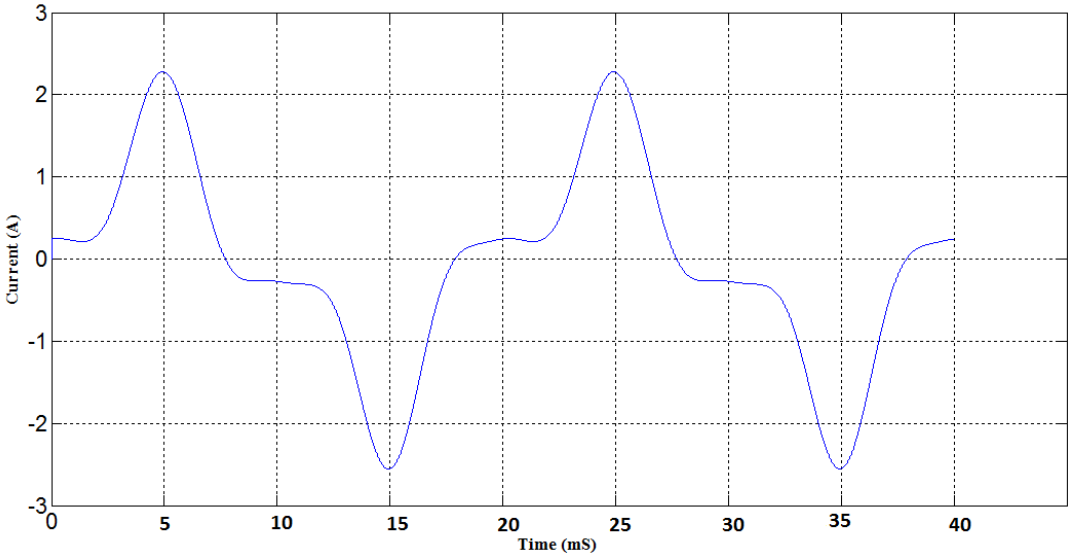

Figure 4.4: Simulated magnetizing current at rated input voltage

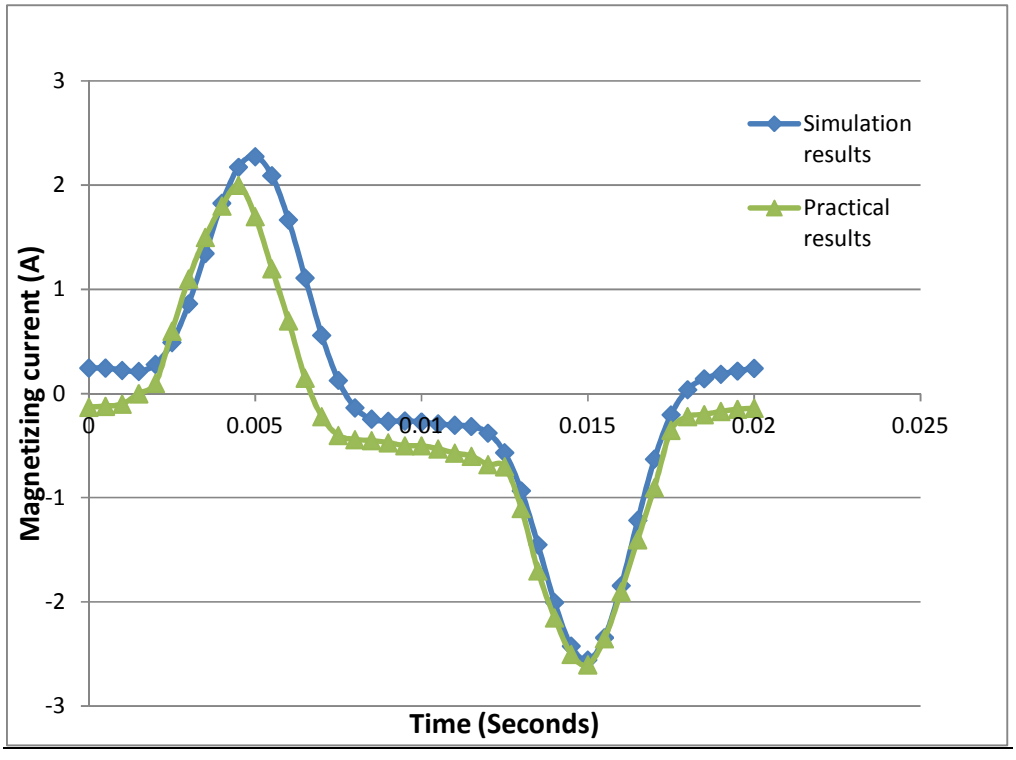

Figure 4.5: Simulated and tested magnetizing current at rated input voltage

4.3 Simulation of primary current on load

Figure 4.6 shows the equivalent circuit corresponding to the test conditions, in which load resistance R_L = 45Ω. This gave a secondary current of 90% of full load secondary current.

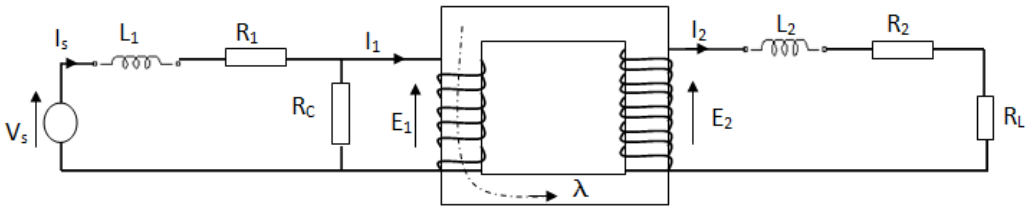

Figure 4.6: Simulated transformer equivalent circuit

Mathematical expressions for the model are,

$$V_s = L_1 \frac{dI_s}{dt} + R_1 I_s + E_1 \quad [4.14]$$

$$E_1 = R_c(I_s - I_1) \quad [4.15]$$

$$E_1 = \frac{d\lambda}{dt} \quad [4.16]$$

$$I_1 - nI_2 = \left(-0.4746\lambda^6 + 2.0944\lambda^5 + 0.7191\lambda^4 - 0.6226\lambda^3 - 0.2973\lambda^2 + 0.0999\lambda - 0.014\right) \quad [4.17]$$

$$E_2 = nE_1 = L_2 \frac{dI_2}{dt} + (R_2 + R_L)I_2 \quad [4.18]$$

Where, *n* is secondary to primary turns-ratio. Rearranged equations are,

$$I_1 = nI_2 + \left(-0.4746\lambda^6 + 2.0944\lambda^5 + 0.7191\lambda^4 - 0.6226\lambda^3 - 0.2973\lambda^2 + 0.0999\lambda - 0.014\right) \quad [4.19]$$

$$L_1 \frac{dI_s}{dt} = V_s - (R_1 + R_c)I_s + R_c I_1 \quad [4.20]$$

$$L_2 \frac{dI_2}{dt} = nR_c(I_s - I_1) - (R_2 + R_L)I_2 \quad [4.21]$$

$$\frac{d\lambda}{dt} = R_c(I_s - I_1) \quad [4.22]$$

Iteration equations corresponding to equations 4.19 to 4.22 are,

$$V_s(k) = V_m \cos(k\omega\delta t) \quad [4.23]$$

$$I_1(k) = nI_2(k) - 0.4746\lambda^6(k) + 2.0944\lambda^5(k) + 0.7191\lambda^4(k) - 0.6226\lambda^3(k) - 0.2973\lambda^2(k) + 0.0999\lambda(k) - 0.014 \quad [4.24]$$

$$I_s(k+1) = I_s(k)\left(1 - \frac{\delta t\,(r_1 + R_c)}{L_1}\right) + \frac{\delta t\, V_s(k)}{L_1} + \frac{\delta t\, R_c I_1(k)}{L_1} \quad [4.25]$$

$$I_2(k+1) = I_2(k)\left(1 - \frac{\delta t\,(R_2 + R_L)}{L_2}\right) + \frac{\delta t\, nR_c(I_s(k) - I_1(k))}{L_2} \quad [4.26]$$

$$\lambda(k+1) = \lambda(k) + \delta t\, R_c\big(I_s(k) - I_1(k)\big) \quad [4.27]$$

Where,
n $= 40/23$
V_m $= 340$ V
$I_s(0) = 0$
$I_2(0) = 0$
$\lambda(0) = 0$, because V_s is selected as a cosωt function
δt $= 0.1$ µs

Iteration equations in 4.23 to 4.27 were simulated in Matlab, and the program code is given in the Appendix (Table A.2). The waveforms of simulated primary current (I_s) and input voltage are shown in Figure 4.7 and Figure 4.8 respectively, corresponding to rated input voltage of 230 V. Figure 4.9 shows the waveforms of the simulated primary current and the tested primary current (given in Figure 3.7) both together for comparisons and two indicate a very close match. This is again a clear evidence of the validity of the model used.

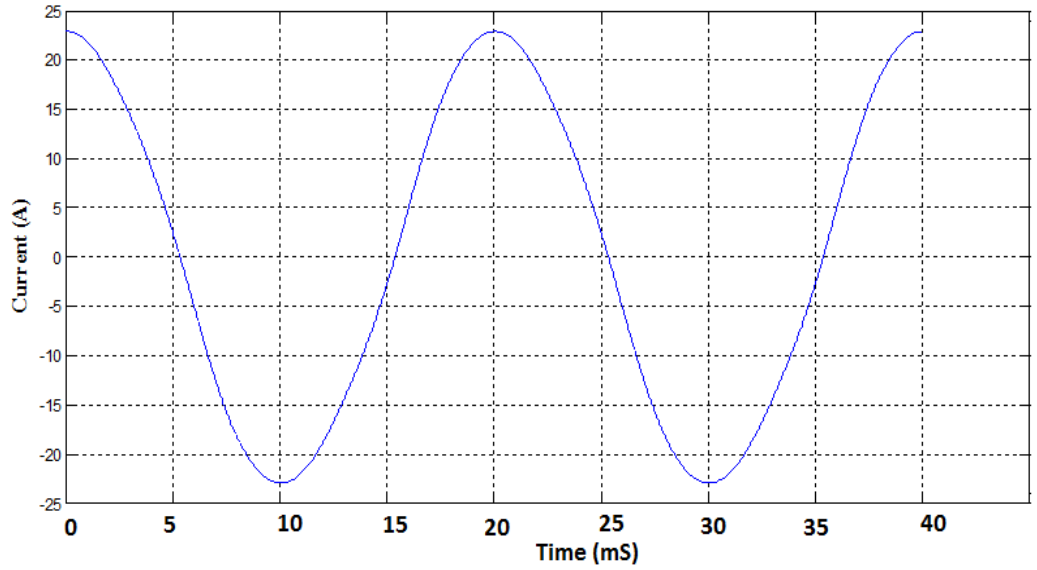

Figure 4.7: Simulated primary current with 90% load (resistive) at rated voltage

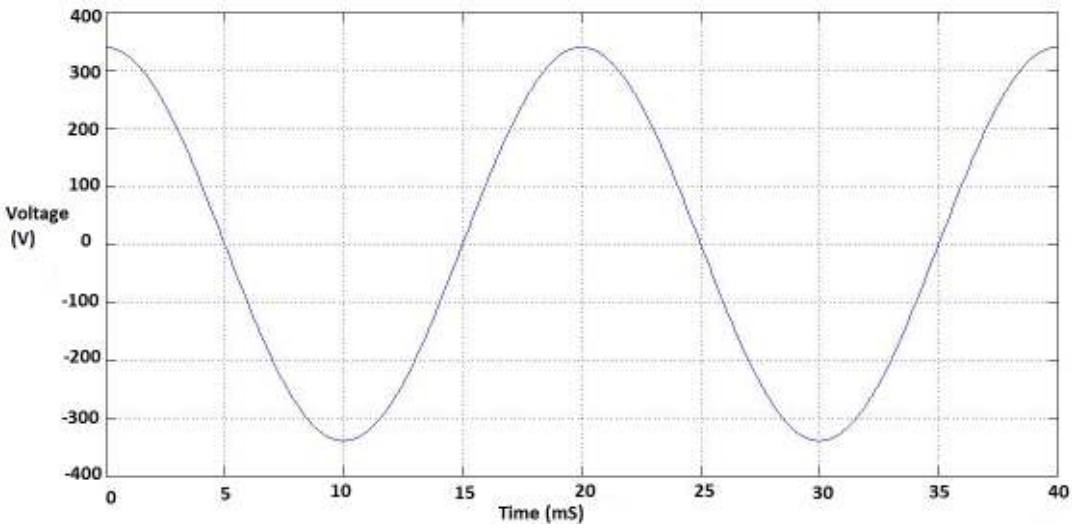

Figure 4.8: Input voltage for the case of 90% load (resistive)

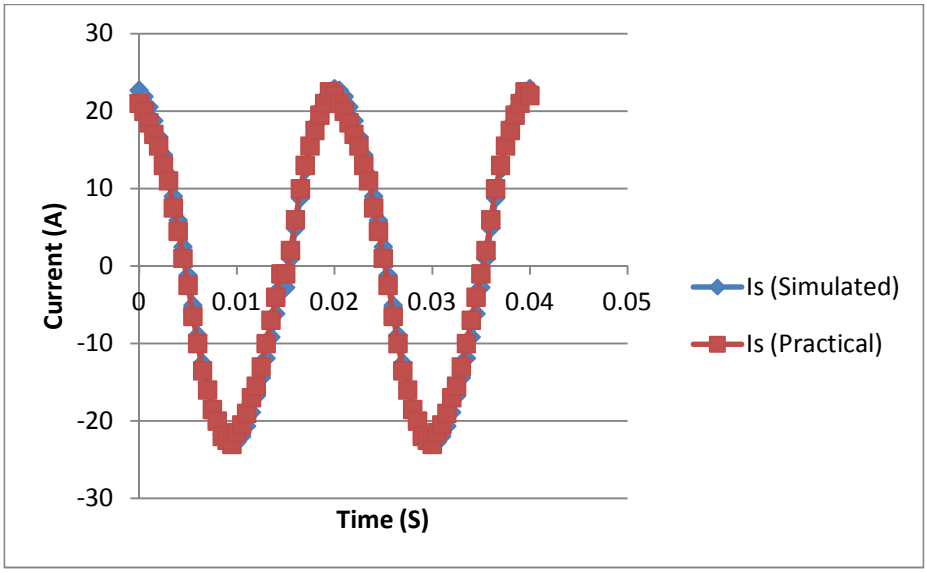

Figure 4.9: Simulated and tested primary current with 90% load (resistive) at rated input voltage

4.4 Simulation of primary current on load with heavy DC current injected to the secondary

Figure 4.10 shows the equivalent circuit used to simulate input current under heavy DC current component in the secondary, which is corresponding to the practical test circuit given in Figure 3.8. Load resistance R_L is set to 45Ω and the resulting secondary current contained a DC component of 40% rated current under rated voltage conditions.

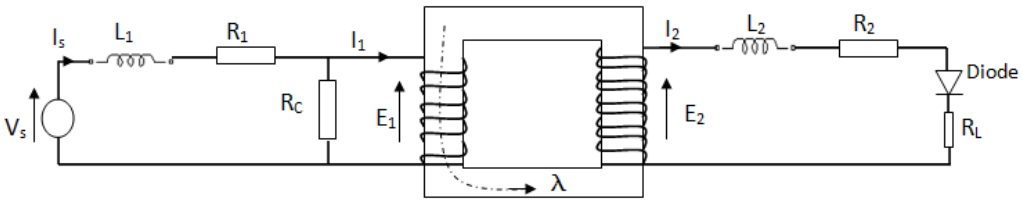

Figure 4.10: Simulated transformer equivalent circuit

Mathematical model for the transformer under these conditions is as follows.

$$V_s = L_1 \frac{dI_s}{dt} + R_1 I_s + E_1 \quad [4.28]$$

$$E_1 = R_c(I_s - I_1) \quad [4.29]$$

$$E_1 = \frac{d\lambda}{dt} \quad [4.30]$$

$$I_1 - nI_2 = \left(-0.4746\lambda^6 + 2.0944\lambda^5 + 0.7191\lambda^4 - 0.6226\lambda^3 - 0.2973\lambda^2 + 0.0999\lambda - 0.014\right) \quad [4.31]$$

$$E_2 = nE_1 = L_2 \frac{dI_2}{dt} + (R_2 + R_L)I_2 \ , I_2 \geq 0 \text{ only} \quad [4.32]$$

Where, *n* is secondary to primary turns-ratio.
Rearranged equations are,

$$I_1 = nI_2 + \left(-0.4746\lambda^6 + 2.0944\lambda^5 + 0.7191\lambda^4 - 0.6226\lambda^3 - 0.2973\lambda^2 + 0.0999\lambda - 0.014\right) \quad [4.33]$$

$$L_1 \frac{dI_s}{dt} = V_s - (R_1 + R_c)I_s + R_c I_1 \quad [4.34]$$

$$L_2 \frac{dI_2}{dt} = nR_c(I_s - I_1) - (R_2 + R_L)I_2 \ , I_2 \geq 0 \text{ only} \quad [4.35]$$

$$\frac{d\lambda}{dt} = R_c(I_s - I_1) \quad [4.36]$$

Iteration equations corresponding to equations 4.33 to 4.36 are,

$$V_s(k) = V_m \cos(k\omega\delta t) \quad [4.37]$$

$$I_1(k) = nI_2(k) - 0.4746\lambda^6(k) + 2.0944\lambda^5(k) + 0.7191\lambda^4(k) - 0.6226\lambda^3(k) - 0.2973\lambda^2(k) + 0.0999\lambda(k) - 0.014 \quad [4.38]$$

$$I_s(k+1) = I_s(k)\left(1 - \frac{\delta t\ (r_1 + R_c)}{L_1}\right) + \frac{\delta t\ V_s(k)}{L_1} + \frac{\delta t\ R_c I_1(k)}{L_1} \quad [4.39]$$

$$I_2(k+1) = I_2(k)\left(1 - \frac{\delta t\ (R_2 + R_L)}{L_2}\right) + \frac{\delta t\ nR_c(I_s(k) - I_1(k))}{L_2} \quad [4.40]$$

$$I_2(k+1) = 0, \text{if } I_2(k+1) < 0 \quad [4.41]$$

$$\lambda(k+1) = \lambda(k) + \delta t\ R_c\left(I_s(k) - I_1(k)\right) \quad [4.42]$$

Where,

$n \quad = 40/23$

$V_m \quad = 340$ V

$I_s(0) = 0$

$I_2(0) = 0$

$\lambda(0) = -1.29$, according to the magnetization characteristic in Figure 4.3, a 40% DC current amounts to an initial flux linkage near -1.29 with V_s selected as a cosωt function

$\delta t \quad = 0.1$ µs

Iteration equations 4.37 to 4.42 were simulated in Matlab, and the program code is given in the Appendix (Table A.3). The waveforms of simulated primary current (I_s) and input voltage are shown in Figure 4.11 and Figure 4.12 respectively, corresponding to rated input voltage of 230 V. Figure 4.13 shows the waveforms of the simulated primary current and the tested primary current (given in Figure 3.9) both together for comparisons and two indicate a very close match. This is again a clear evidence of the validity of the model used. Figure 4.14 shows the simulated input current waveform together with the input voltage and the graph shows how the positive half-cycle of current becomes inphase with the voltage, and negative half-cycles get lagging nearly 90° behind the voltage.

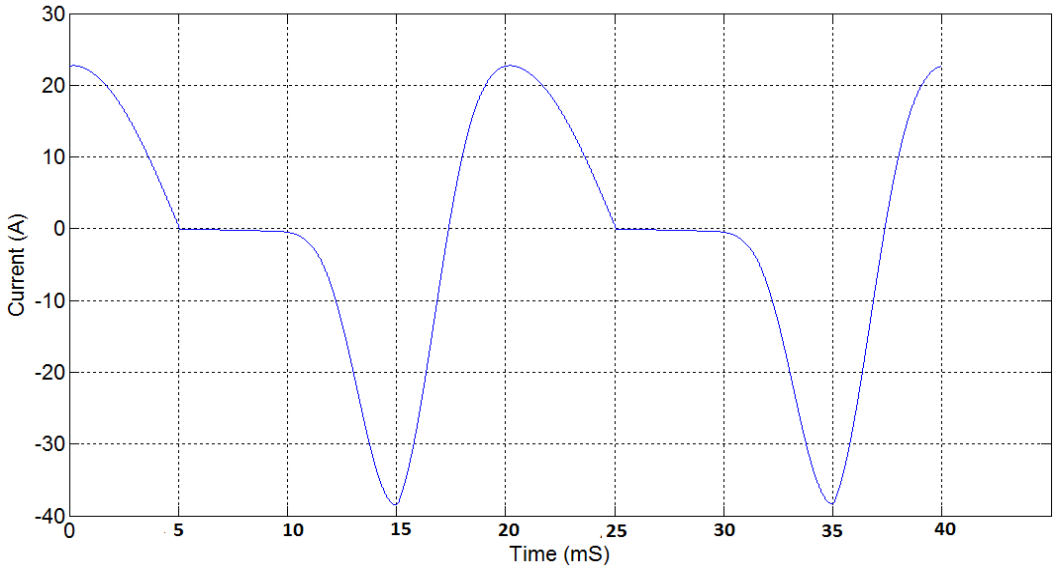

Figure 4.11: Simulated primary current with 40% DC current in the secondary, created by rectification of 90% full load (resistive) current at rated input voltage

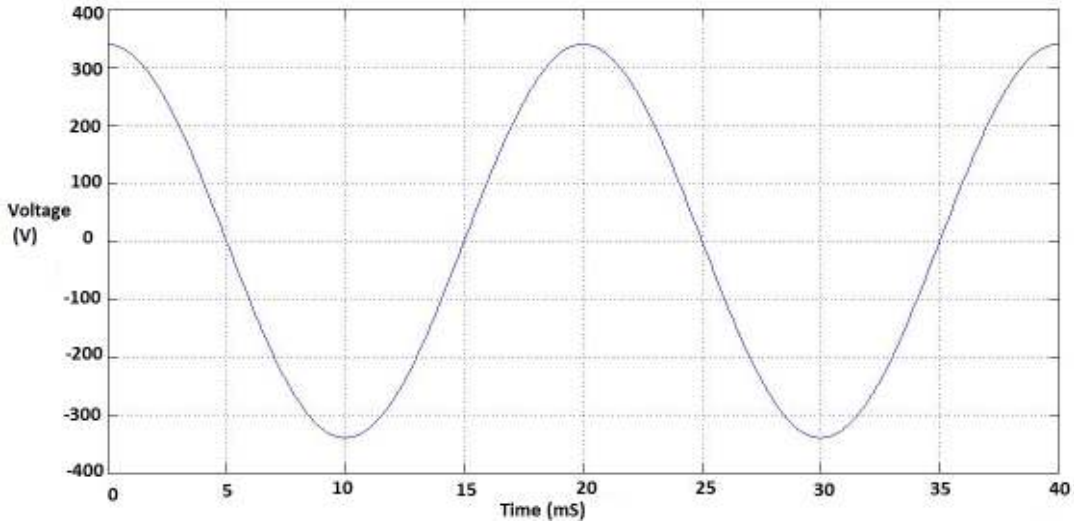

Figure 4.12: Input voltage for the case of with 40% DC current in the secondary

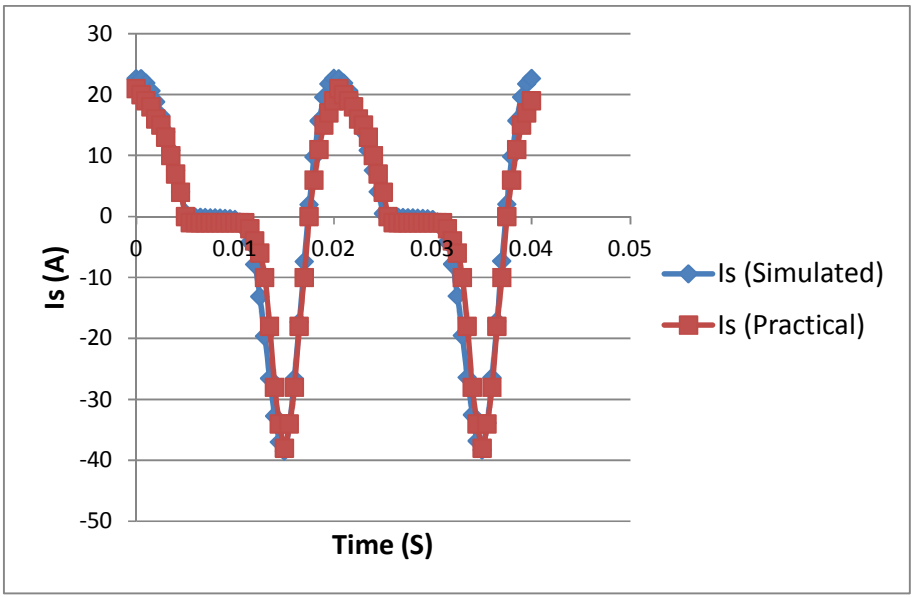

Figure 4.13: Simulated and tested input current with 40% DC current at the secondary, created by rectification of 90% full load (resistive) current at rated input voltage

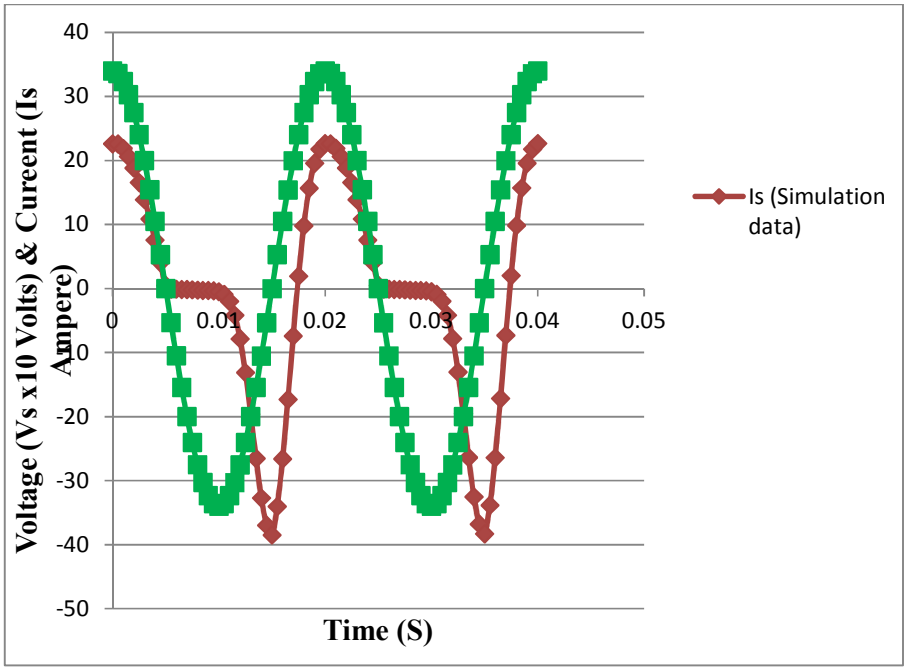

Figure 4.14: Simulated input current and voltage with 40% DC current at the secondary, created by rectification of 90% full load (resistive) current at rated input voltage

4.5 Simulation of primary current on load with small DC current injected to the secondary

Figure 4.15 shows the equivalent circuit used to simulate input current when the secondary side is injected with a small DC current. This circuit is corresponding to the practical test described in figure 3.10, where DC current component in the secondary was created by rectifying part of the load current. Resulting DC current component is 10% rated current with the AC current component amounting to nearly 90% rated current. Input voltage is 230 V across the primary.

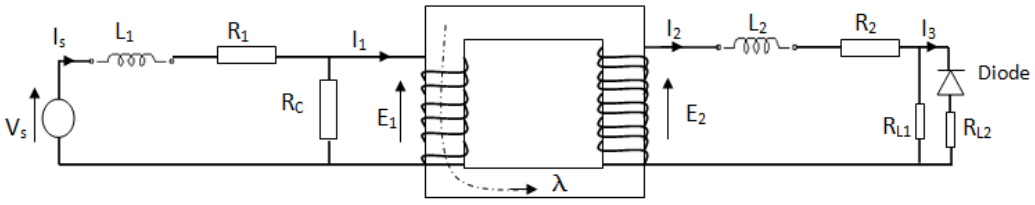

Figure 4.15: Simulated transformer equivalent circuit with small DC current

Mathematical equations corresponding to the model are,

$$V_s = L_1 \frac{dI_s}{dt} + R_1 I_s + E_1 \quad [4.43]$$

$$E_1 = R_c(I_s - I_1) \quad [4.44]$$

$$E_1 = \frac{d\lambda}{dt} \quad [4.45]$$

$$I_1 - nI_2 = \left(-0.4746\lambda^6 + 2.0944\lambda^5 + 0.7191\lambda^4 - 0.6226\lambda^3 - 0.2973\lambda^2 + 0.0999\lambda - 0.014\right) \quad [4.46]$$

$$I_3 = \left(\frac{R_{L1}}{R_{L1} + R_{L2}}\right) I_2, \quad I_3 \leq 0 \text{ only} \quad [4.47]$$

$$E_2 = nE_1 = L_2 \frac{dI_2}{dt} + R_2 I_2 + R_{L1}(I_2 - I_3) \quad [4.48]$$

Where, *n* is secondary to primary turns-ratio.
Rearranged equations are,

$$I_1 = nI_2 + \left(-0.4746\lambda^6 + 2.0944\lambda^5 + 0.7191\lambda^4 - 0.6226\lambda^3 - 0.2973\lambda^2 + 0.0999\lambda - 0.014\right) \quad [4.49]$$

$$L_1 \frac{dI_s}{dt} = V_s - (R_1 + R_c) I_s + R_c I_1 \quad [4.50]$$

$$L_2 \frac{dI_2}{dt} = nR_c(I_s - I_1) - R_2 I_2 - R_{L1}(I_2 - I_3) \quad [4.51]$$

$$I_3 = \left(\frac{R_{L1}}{R_{L1} + R_{L2}}\right) I_2, \quad I_3 \leq 0 \text{ only} \quad [4.52]$$

Iteration equations corresponding to equations 4.49 to 4.52 are,

$$V_s(k) = V_m \cos(k\omega\delta t) \quad [4.53]$$

$$I_1(k) = nI_2(k) - 0.4746\lambda^6(k) + 2.0944\lambda^5(k) + 0.7191\lambda^4(k) - 0.6226\lambda^3(k) - 0.2973\lambda^2(k) + 0.0999\lambda(k) - 0.014 \quad [4.54]$$

$$I_s(k+1) = I_s(k)\left(1 - \frac{\delta t\,(r_1 + R_c)}{L_1}\right) + \frac{\delta t\, V_s(k)}{L_1} + \frac{\delta t\, R_c I_1(k)}{L_1} \quad [4.55]$$

$$I_2(k+1) = I_2(k)\left(1 - \frac{\delta t\ (R_2 + R_{L1})}{L_2}\right) + \frac{\delta t\ nR_c(I_s(k) - I_1(k))}{L_2} + \frac{\delta t\ R_{L1} I_3(k)}{L_2} \quad [4.56]$$

$$I_3(k+1) = I_2(k+1)\left(\frac{R_{L1}}{R_{L1} + R_{L2}}\right) \quad [4.57]$$

$$I_3(k+1) = 0, \qquad \text{if } I_2(k+1) > 0 \quad [4.58]$$

$$\lambda(k+1) = \lambda(k) + \delta t\ R_c\big(I_s(k) - I_1(k)\big) \quad [4.59]$$

Where,

n $= 40/23$

V_m $= 340$ V

$I_s(0) = 0$

$I_2(0) = 0$

$I_3(0) = 0$

$\lambda(0)$ $= 1.04$, according to the magnetization characteristic in Figure 4.3, a 10% DC current (in reverse direction) amounts to an initial flux linkage near 1.04 with V_s selected as a cosωt function

δt $= 0.1$ μs

Iteration equations 4.53 to 4.59 were simulated in MATLAB, and the program code is given in the Appendix (Table A.4). The waveforms of simulated primary current (I_s) and input voltage are shown in Figure 4.16 and Figure 4.17 respectively, corresponding to rated input voltage of 230 V. Figure 4.18 shows the waveforms of the simulated primary current and the tested primary current (given in Figure 3.11) both together for comparisons and two indicate a very close match. This is again a clear evidence of the validity of the model used. Figure 4.19 shows the simulated input current waveform together with the input voltage and the graph shows how the positive and negative half-cycles of current have become asymmetric, i.e. how the positive half-cycle has broaden and negative half cycle narrowed.

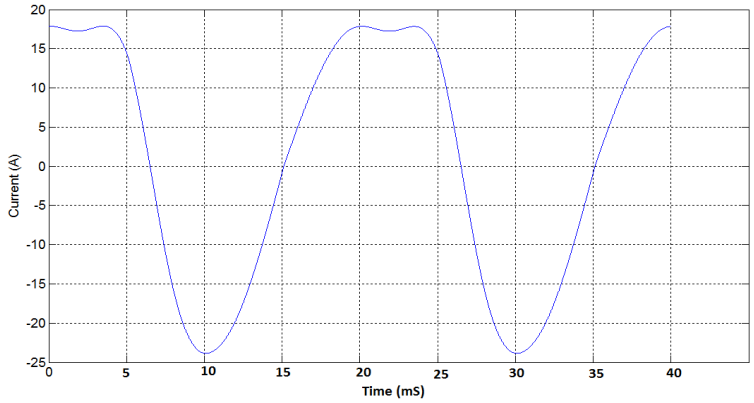

Figure 4.16: Simulated input current with 10% DC current at 90% load (resistive) at rated input voltage

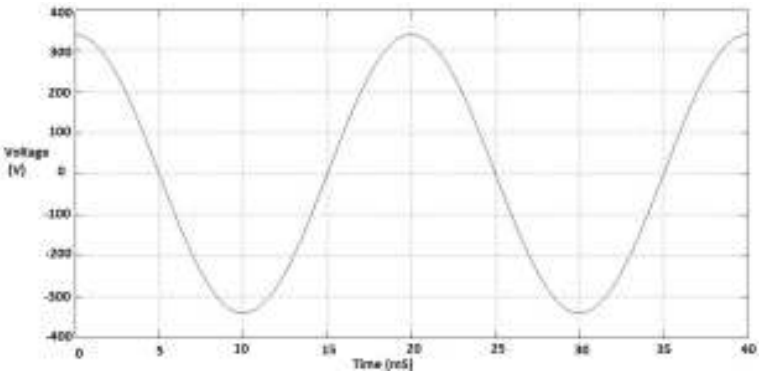

Figure 4.17: Simulated input voltage for the case of 10% DC current at 90% load (resistive)

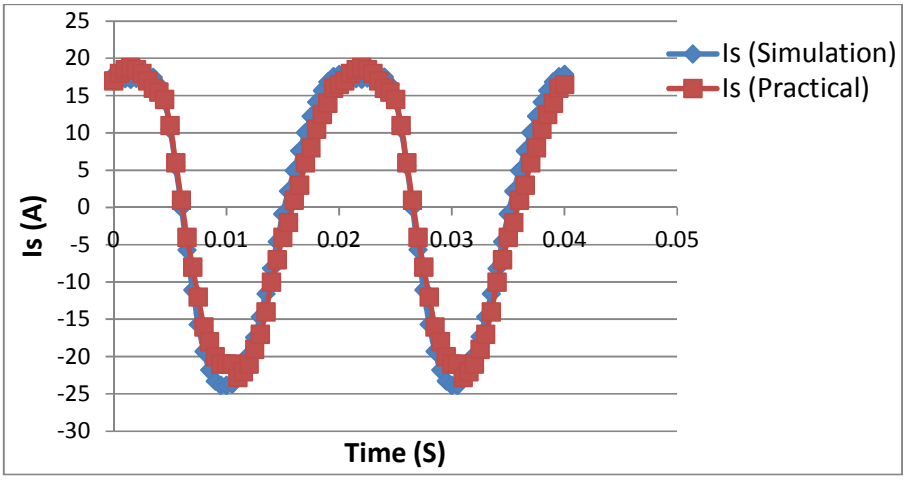

Figure 4.18: Simulated and tested input current with 10% DC current at 90% load (resistive) at rated input voltage

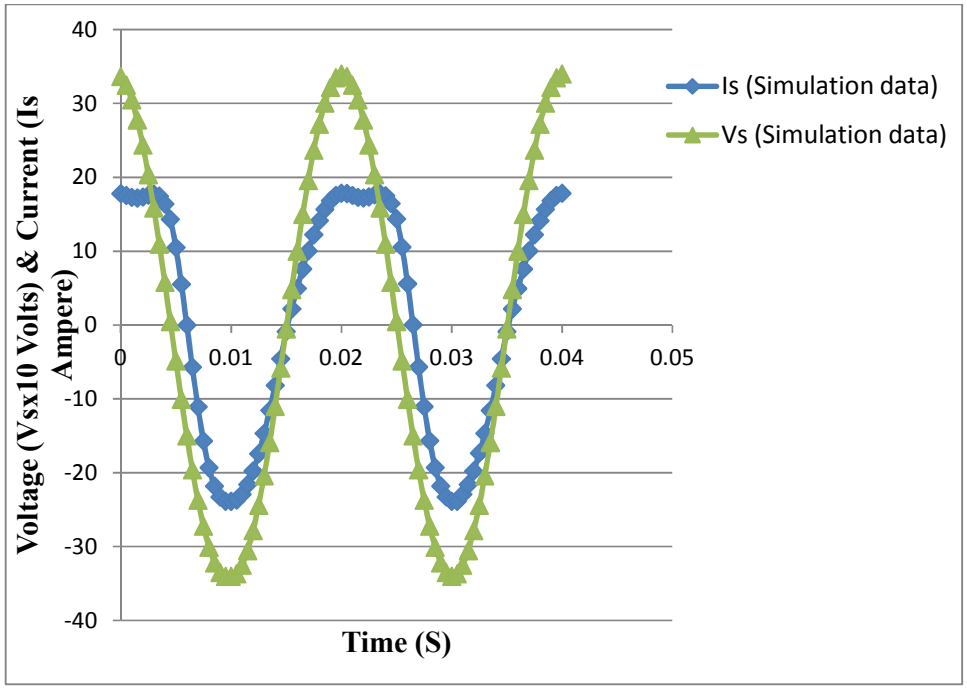

Figure 4.19: Simulated input current and voltage with 10% DC current at 90% load (resistive) at rated input voltage

The results of the simulations of practical test conditions, each, indicate extreme closeness of agreement with the observed waveform. This is a sufficient proof of the validity of the developed-model. The model is comprehensive enough to study the transformer under any operating conditions, other than studying the behaviour under load injected DC current. This is a significant milestone of achievement in the circumstances of not having such a model in commonly used simulation packages.

CHAPTER 5

PROPOSED SYSTEM OF ELIMINATING DC CURRENT AT THE POINT OF COMMON COUPLING (PCC)

5.1 System Overview

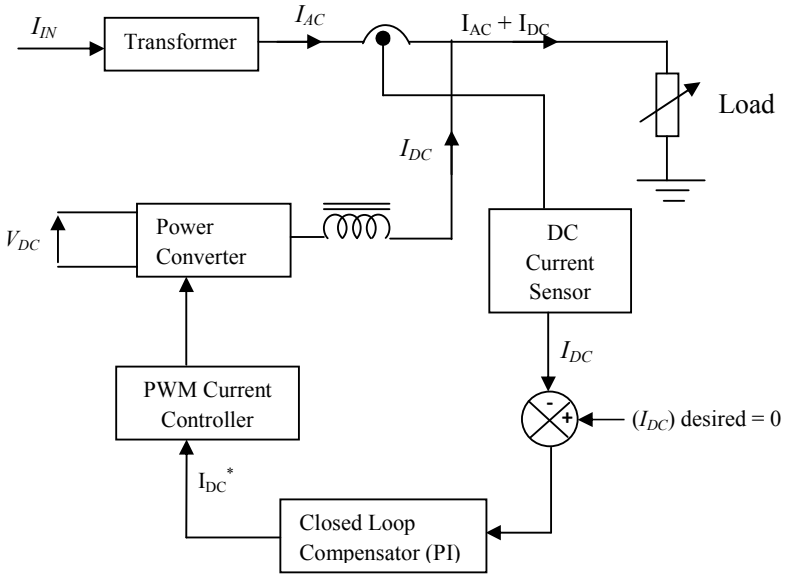

Figure 5.1: Proposed arrangement of DC current cancellation system at PCC

Figure 5.1 is an overview of the proposed system of eliminating DC current in each phase of the transformer. DC current created by the consumer-loads is sensed at the transformer secondary by a DC-current sensor and the information is directed to a closed loop current controller, which steers a power electronic converter with PWM control to deliver an equal DC current to the load. This way, the DC current circulating in the transformer secondary is eliminated.

5.2 DC Current Sensor

Detecting a very small DC current superimposed with a large AC current is difficult and lead to inaccuracies unless a proper sensing method is used. Direct sensing of current using typical current sensors, such as Hall-sensors, does not guarantee the

required accuracy because the inherent non-linearity and drift effects can distort the information of the superimposed DC current.

Voltage can be sensed more accurately than current and hence a voltage sensing based approach was considered more appropriate in the proposed system. Any DC current flowing in the transformer secondary creates a corresponding DC voltage component across the secondary-resistance, so by measuring the secondary voltage, it is possible to extract this DC component easily.

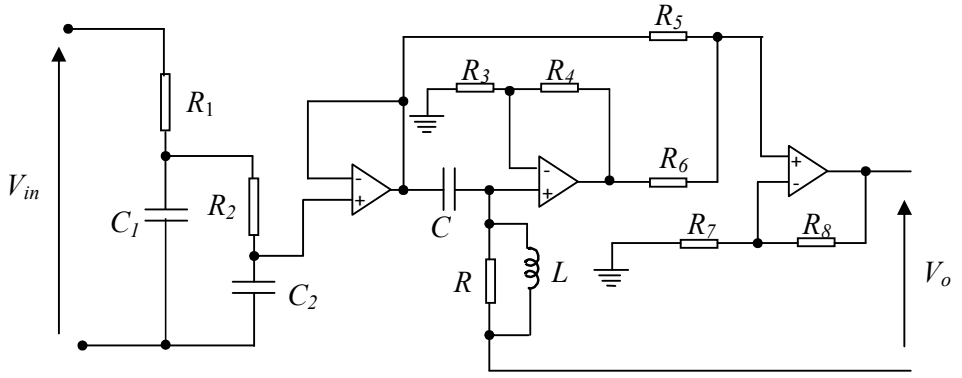

Figure 5.2: DC current detector circuit

Figure 5.2 shows the arrangement of the proposed DC current sensor. At the front end, it uses a two-stage *RC*-divider to attenuate the AC voltage component in the measuring-voltage without affecting the magnitude of the superimposed DC component. Values of *R* and *C* components in the voltage divider were designed to lower the AC component from 400 V down to about 2 V with a response time near 0.5 second. The residual AC voltage component present in the output of the RC divider is then removed by an active low-pass filter to separate the DC component.

Signal output from the RC divider stage was buffered before passing it on to the active low pass filter. This was done for the safety of the filter hardware and also to avoid the signal itself becoming distorted due to the loading by the filter.

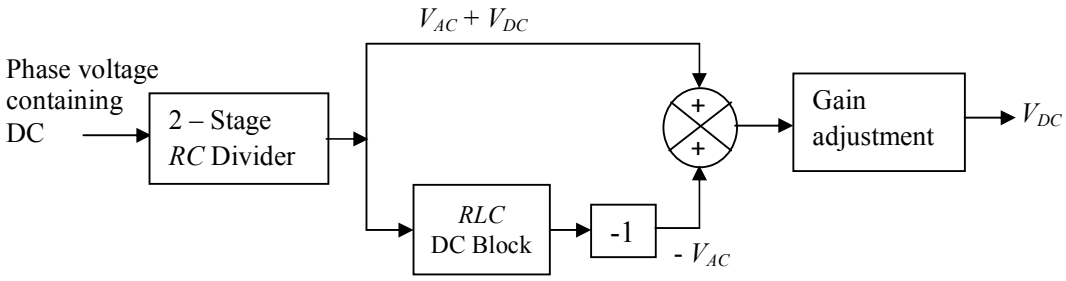

Figure 5.3: Functionality of DC current detector

Figure 5.3 shows the functionality of the current sensor. The active low pass filter takes its input signal along two parallel paths. In one path, the DC component in the signal is dropped and -1 gain is given to the remaining signal. The signals so arriving on two paths are added together so that the output becomes the DC component only. Positive gain stage at the end restores the magnitude of the output to match it with the actual DC voltage present at the input against slight attenuations, if any.

5.2.1 Transfer Function of DC Current Sensor

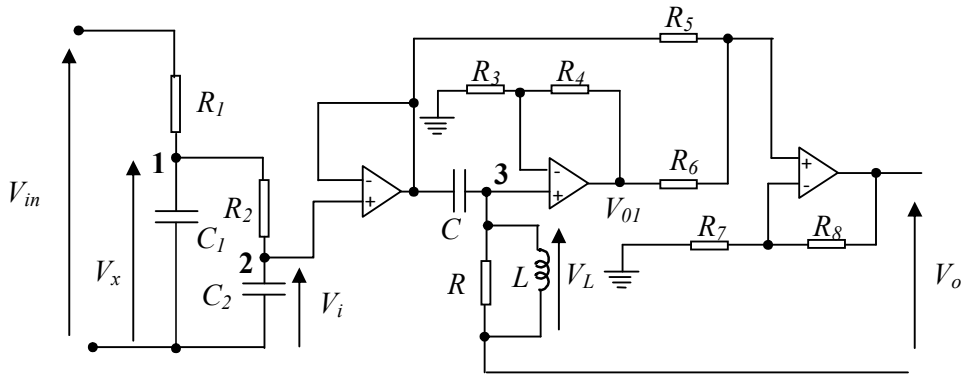

Figure 5.4: DC current detector circuit

Applying Kirchoff's Current Law to node-1 and node-2,

$$\frac{V_{in} - V_x}{R_1} = V_x.SC_1 + \frac{V_x - V_i}{R_2} \quad [5.1]$$

$$\frac{V_i - V_x}{R_2} + V_i.SC_2 = 0 \quad [5.2]$$

Eliminating V_x from equations 5.1 and 5.2, the transfer function $G(S)$ of the *RC*-divider stage is obtained as,

$$G(s) = \frac{V_i}{V_{in}} = \frac{1}{S^2C_1C_2R_1R_2 + S(C_1R_1 + C_2R_2 + C_2R_1) + 1} \quad [5.3]$$

Applying Kirchoff's Current Law to node-*3*,

$$(V_i - V_L).SC = \frac{V_L}{R} + \frac{V_L}{SL} \quad [5.4]$$

For the non-inverting amplifier stage in the *RLC* filter unit,

$$V_{o1} = \left(1 + \frac{R_4}{R_3}\right).V_L \quad [5.5]$$

From equations 5.4 and 5.5, Transfer function $F(S)$ between V_i and V_{o1} is,

$$F(s) = \frac{V_{o1}}{V_i} = \frac{\left(1 + \frac{R_4}{R_3}\right)S^2}{S^2 + \frac{S}{RC} + \frac{1}{LC}} \quad [5.6]$$

For the amplifier of the output stage,

$$V_o = \left(1 + \frac{R_8}{R_7}\right)\left(\frac{V_i + V_{01}}{2}\right) \quad [5.7]$$

From equations 5.3, 5.6 and 5.7, the overall transfer function of the current sensor is found as,

$$\frac{V_o}{V_{in}} = \left(1 + \frac{R_8}{R_7}\right)\left(\frac{1 + F(s)}{2}\right)G(s) \quad [5.8]$$

Values of the current detector components are:

$R_1 = 2\ \text{k}\Omega$	$R_3 = 0.1\ \text{k}\Omega$	$R = 10\ \text{k}\Omega$
$R_2 = 1.669\ \text{k}\Omega$	$R_4 = 168.8\ \text{k}\Omega$	$L = 10\ \text{mH}$
$C_1 = 30\ \mu\text{F}$	$R_5 = 20\ \text{k}\Omega$	$C = 0.6\ \mu\text{F}$
$C_2 = 30\ \mu\text{F}$	$R_6 = 20\ \text{k}\Omega$	
	$R_7 = 20\ \text{k}\Omega$	
	$R_8 = 24.6\ \text{k}\Omega$	

Substituting values,

$$1 + \frac{R_8}{R_7} = 2.23$$

$$F(s) = \frac{1689S^2}{S^2 + 166.7S + 166666666.7}$$

$$G(s) = \frac{1000}{3S^2 + 170S + 1000}$$

$$\frac{V_o}{V_{in}} = \frac{1116(1690S^2 + 166.7S + 166666666.7)}{(S^2 + 166.7S + 166666666.7)(3S^2 + 170S + 1000)}$$

Transfer function *F*(*S*) represents the gain of the path of *RLC* branch of the active low pass filter. Its value at $S = 0$ gives the DC gain and at $S = j2\pi \times 50$ rad/s gives the 50 Hz gain. By substituting values they are found as,

$F(0) = 0$
$F(j2\pi \times 50) = (-1.00 + \text{j}0.00)$

Thus, the specifications of zero gain for the DC and -1 gain for the 50 Hz signal are satisfied.

5.2.2 Response of the DC current sensor

DC current sensor circuit was simulated in MATLAB and a series of tests were conducted to assess the sensor response.

Practical capacitors, especially two 30 µF capacitors used in the *RC* divider stage have some leakage resistances that act to attenuate the DC signal output, slightly. To account for this effect a leakage resistance of 53 kΩ, which is typical for a 30 µF capacitor, was used across each capacitor in the simulation. This enabled a better adjustment of the gain of final stage of the sensor to trim out stray effects and obtain

correct magnitude of the sensor output equal to the actual DC voltage superimposed in the transformer secondary.

Figure 5.5 shows the simulation model with a step input of 1.25 V (DC) on top of 400 V (AC) at the input, and Figure 5.6 shows the corresponding response of the current sensor. The response shows a transient peak and this is solely due to the AC voltage at the input, which is a disturbance. When modeling feedback current controller transfer functions, this AC voltage driven transient is considered as a disturbance on sensor output.

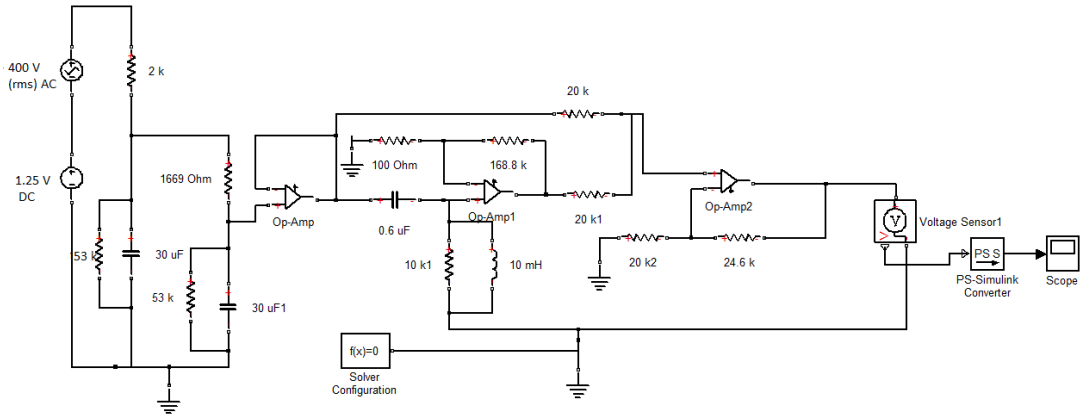

Figure 5.5: MATLAB simulation model with 1.25 V (DC) on top of 400 V (AC) at sensor input

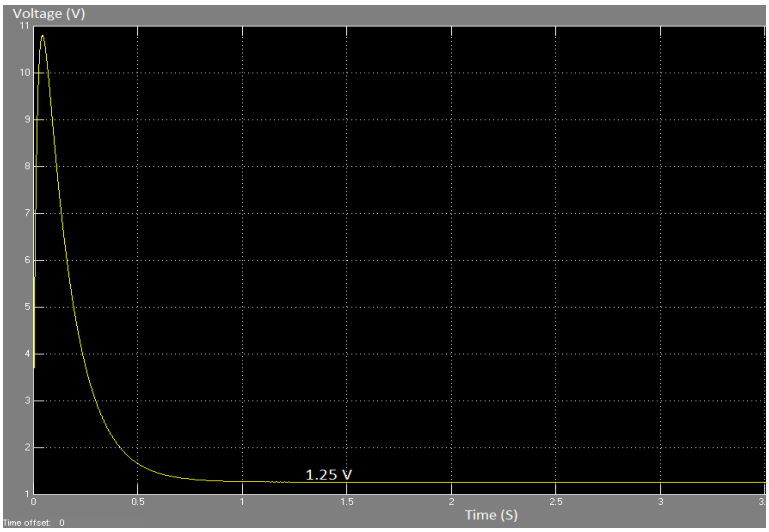

Figure 5.6: Response of the current Sensor for step input of1.25 V DC superimposed with 400 V (AC)

Figure 5.7 shows the step response of the current sensor for 1.25 V (DC) input without AC voltage at the input. It can be observed that the response is also a step, coinciding with the input. This is a special feature of this sensor. Initial delay introduced to the response by the RC divider is subsequently restored by the active low pass filter which sees transient variations on the output of RC divider as an AC signal component and remove it accordingly.

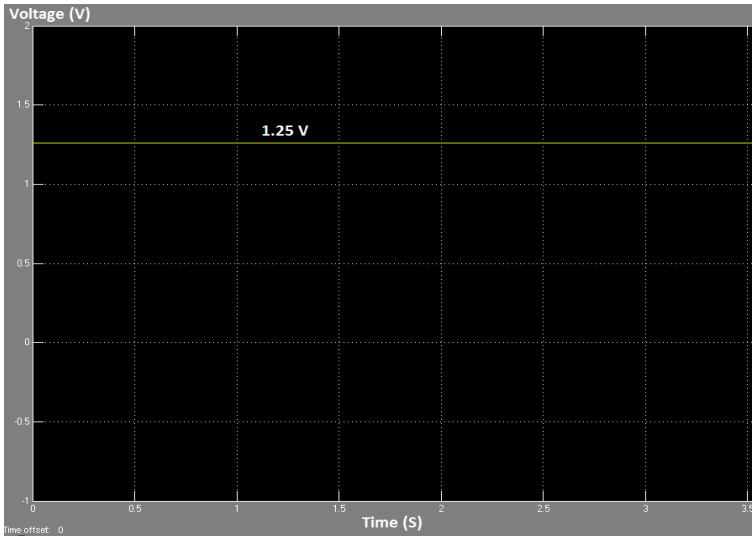

Figure 5.7: Sensor output for 1.25 V DC step input without AC

5.3 Power Electronic Converter

The function of power electronic converter is to inject DC current in to the transformer secondary, as requested by the closed loop controller. Injection is done phase-wise and hence the standard H-bridge configured power converter arrangement, shown in Figure 5.8, was considered adequate. To ensure satisfactory injection of current against the AC voltage present at the transformer secondary, the required DC voltage input to the converter should be sufficiently greater than the peak value of the AC voltage at the secondary. The 1-phase transformer used in this study had a secondary voltage of 400 V (rms) and hence 660 V (DC) voltage input was selected to give an adequate margin.

An inductor *L* between the output of the converter and the transformer secondary is a must to enable the control of current. Inductance of the required inductor depends on the DC voltage chosen for the converter, and the limits of switching frequency (or ripple amplitude in current output) specified for the converter. For a given DC voltage, if the inductance is made lower, the switching frequency (or current ripple amplitude) will rise significantly. Higher switching frequency is not desirable owing to higher losses, and higher ripple in current is not acceptable because it directly affects the quality of the total current elimination exercise.

Between the switching frequency and the ripple amplitude, one can be fixed up while the other is allowed to vary by the choice of the current control strategy. For example, Hysteresis Current Control strategy can fixed up the ripple amplitude, and the switching frequency is determined by the combination of DC voltage and the inductance; carrier based current control strategy can fix up the switching frequency, and the ripple amplitude is determined by the combination of DC voltage and inductance.

Hysteresis Current Control strategy with current ripple amplitude fixed up at 0.02 A (peak-peak) was decided for the implementation. Then, an inductance of 1 H was found to be satisfactory for the 660V DC input, which could limit switching frequency between 16.7 kHz and 4.6 kHz.

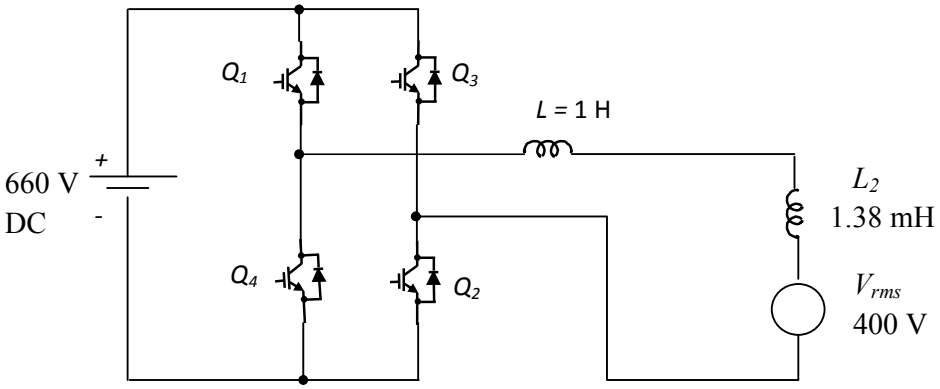

Figure 5.8: Circuit of Power Electronic Converter

5.3.1 Switching frequency range for the Power Electronic Converter

At any instant of time, switching Q_1 & Q_2 pair causes the current I to rise, and switching Q_3 & Q_4 pair makes the current to fall. Switchover between the two pairs occurs rapidly so that current is kept within ± 0.01A tolerance-band around the desired I, adaptively.

Minimum switching frequency occurs at the positive or negative peak of the AC voltage waveform, i.e at point *A* or point *C* of the waveform shown in the figure 5.9. Maximum switching frequency occurs at the zero crossing points of the AC voltage waveform, i.e. at point *B* of the AC voltage waveform.

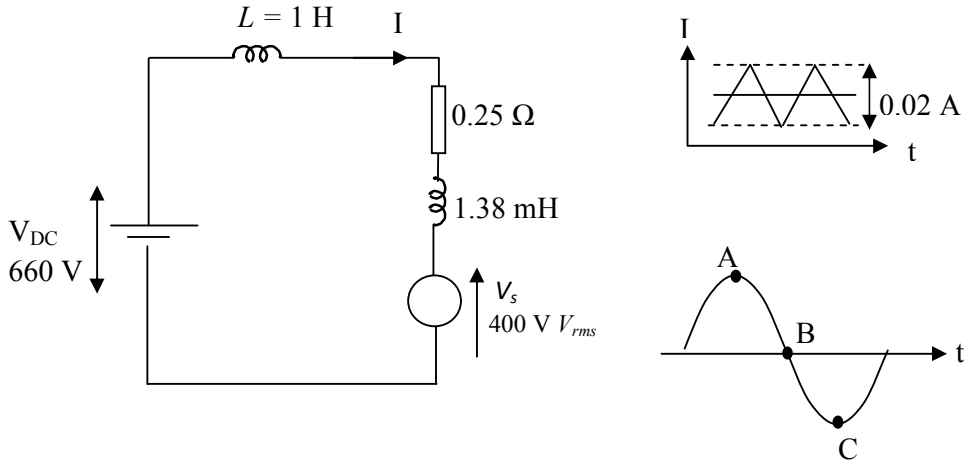

Figure 5.9: Equivalent power-circuit of the DC injection system

At minimum switching frequency points,

$$\frac{dI}{dt} = \frac{V_L}{L}$$

$$\therefore \frac{dI}{dt} = \begin{cases} \dfrac{660 - 400\sqrt{2}}{1} = 100 \ {}^{\mathrm{A}}/_{\mathrm{S}}, & \text{while } \mathrm{Q_1} \& \ Q_2 \text{ pair is ON} \\ \dfrac{-660 - 400\sqrt{2}}{1} = -1220 \ {}^{\mathrm{A}}/_{\mathrm{S}}, & \text{while } \mathrm{Q_3} \& \ Q_4 \text{ pair is ON} \end{cases} \qquad [5.9]$$

Time δt taken for current to change by 0.02 A in the tolerance band, according to equation 5.9, is,

$$\delta t = \begin{cases} \frac{0.02}{100}\ \text{s} = 0.200\ \text{ms}, & \text{while } Q_1 \& \ Q_2 \text{ pair is ON} \\ \frac{0.02}{1220}\text{s} = 0.016\ \text{ms}, & \text{while } Q_3 \& \ Q_4 \text{ pair is ON} \end{cases} \quad [5.10]$$

Thus, minimum switching frequency f_{min} , according to equation 5.10,is found as,

$$f_{min} = \frac{1}{(0.2 + 0.016)}\text{kHz} = 4.6\ \text{kHz}$$

Similarly, at maximum switching frequency points,

$$\therefore \frac{dI}{dt} = \begin{cases} \frac{660}{1} = \ 660\ \ {}^{\text{A}}/_{\text{s}}, & \text{while } Q_1 \& \ Q_2 \text{ pair is ON} \\ \frac{-660}{1} = -660\ \ {}^{\text{A}}/_{\text{s}}, & \text{while } Q_3 \& \ Q_4 \text{ pair is ON} \end{cases} \quad [5.11]$$

Time δt taken by current to change by 0.02 A in the tolerance band, according to equation 5.11, is,

$$\delta t = \begin{cases} \frac{0.02}{660}\ \text{s} = 0.030\ \text{ms}, & \text{while } Q_1 \& \ Q_2 \text{ pair is ON} \\ \frac{0.02}{660}\text{s} = 0.030\ \text{ms}, & \text{while } Q_3 \& \ Q_4 \text{ pair is ON} \end{cases} \quad [5.12]$$

Thus, maximum switching frequency f_{max} , according to equation 5.12, is found as,

$$f_{max} = \frac{1}{(0.030 + 0.030)}\text{kHz} = 16.7\ \text{kHz}$$

5.3.2 Transfer Function of Power Electronic Converter

Transfer function of the power electronic converter with hysteresis current control was derived by considering the action of the converter system in converting a step

input at the current controller to the actual current injected to the transformer secondary.

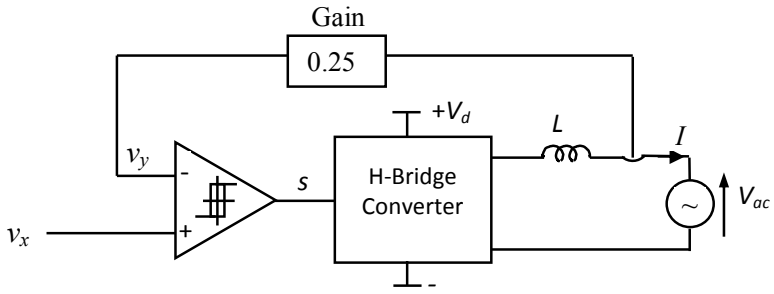

Figure 5.10: Schematics of Power Electronic Converter with Hysteresis Controller function to derive transfer function

v_x = Input to the current controller
v_y = Feedback of output current at the current controller
s = Switching signal to the H-Bridge
I = Current injected to transformer secondary, by the H-Bridge

Figure 5.10 shows the schematic of the hysteresis current controller, power electronic converter, and the transformer secondary. Current feedback from the output of the power converter to the hysteresis-controller was made with a gain of 0.25 because the actual current in the transformer secondary was sensed (by the current sensor) as a voltage drop across the 0.25 Ω secondary-resistance of the transformer.

A step input v_x to the current controller throws the switching signal s HIGH, allowing switch pair Q_1 &Q_2 of the H-bridge to turn-on, and thereby DC voltage V_d to force current I through inductor L, rising linearly with time. AC voltage V_{ac} of the transformer influences the rate of buildup of current during this initial transient but its effect can be ignored in the transfer function model due to V_d being greater than the peak of V_{ac}, and zero mean influence by V_{ac} over its cycle.

Soon after current I reaches the value that makes feedback v_y equal to input v_x, the hysteresis control action begins and, thereafter, the current I will be held at this value, continuously. Therefore, the transfer function of the power electronic converter is

obtained by modelling the initial transient of building current to the value set by the v_x input.

Figure 5.11 shows ideal variation of feedback signal v_y with time for a step input v_x, and Figure 5.12 shows an exponential approximation of the same.

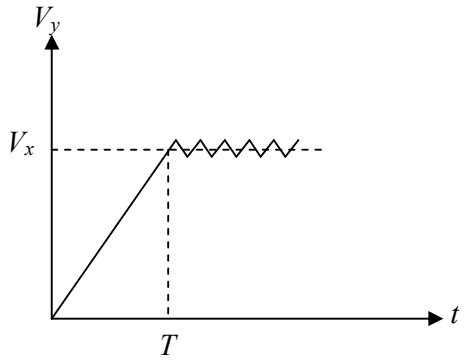

Figure 5.11: Step response of current controller and power electronic converter

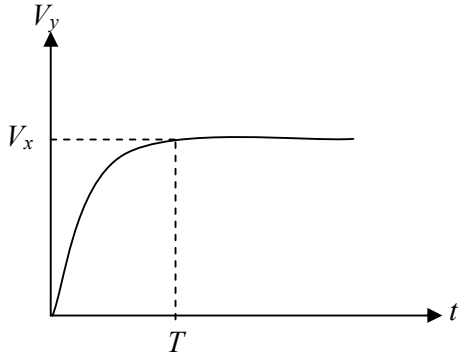

Figure 5.12: Exponential approximation to Step response of current controller and power electronic converter

During the transient, neglecting the influence by the AC voltage at the transformer secondary, and taking k as the feedback gain ($k = 0.25$)

$$\frac{dV_y}{dt} = k\frac{dI}{dt} = k\frac{V_d}{L} \qquad [5.13]$$

Time T for V_y to reach V_x is found, according to equation 5.13, as,

$$T = \frac{L\,V_x}{kV_d} \qquad [5.14]$$

Exponential approximation was made taking its time-constant τ to be one-fourth of the time T to reach steady state (i.e. four-time constant rule). Accordingly,

$$V_y = V_x\,(1 - e^{-t/\tau})$$

$$\therefore F(s) = \frac{V_y(s)}{V_x(s)} = \frac{\frac{1}{\tau}}{\left(s + \frac{1}{\tau}\right)} = \frac{\frac{4}{T}}{\left(s + \frac{4}{T}\right)} = \frac{\frac{4kV_d}{LV_x}}{\left(s + \frac{4kV_d}{LV_x}\right)} \qquad [5.15]$$

$$k = 0.25$$

$V_d = 660\ V$
$L = 1\ H$
$V_x = 0.5$ V (chosen corresponding to a DC injection of 2 A as a representative value)

$$\therefore F(S) = \frac{1320}{(S + 1320)} \qquad [5.16]$$

5.3.3 Response of the Power Electronic Converter

Current-injecting response of the power electronic converter with hysteresis current control was tested by simulating the converter, current controller and the transformer in MATLAB. Figure 5.13 shows the simulation model. Figure 5.14 shows the response of output current for a step input (v_x) to the hysteresis current controller. The response clearly shows that the output current has approximately linear-building transient followed by constant current sustained by the action of hysteresis current controller.

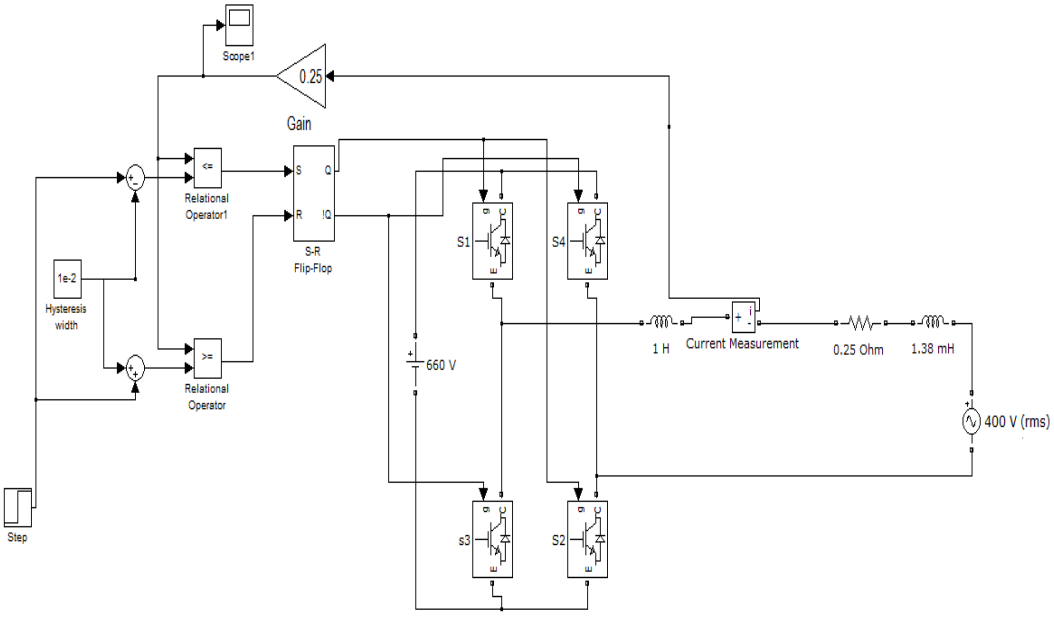

Figure 5.13: MATLAB simulation model of Converter, hysteresis Current controller and transformer

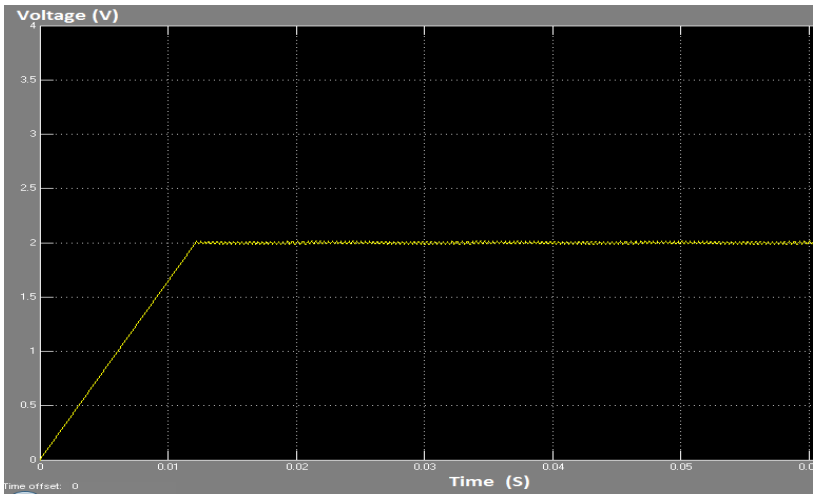

Figure 5.14: Step response of output current of the power electronic converter

5.4 Closed Loop Compensator

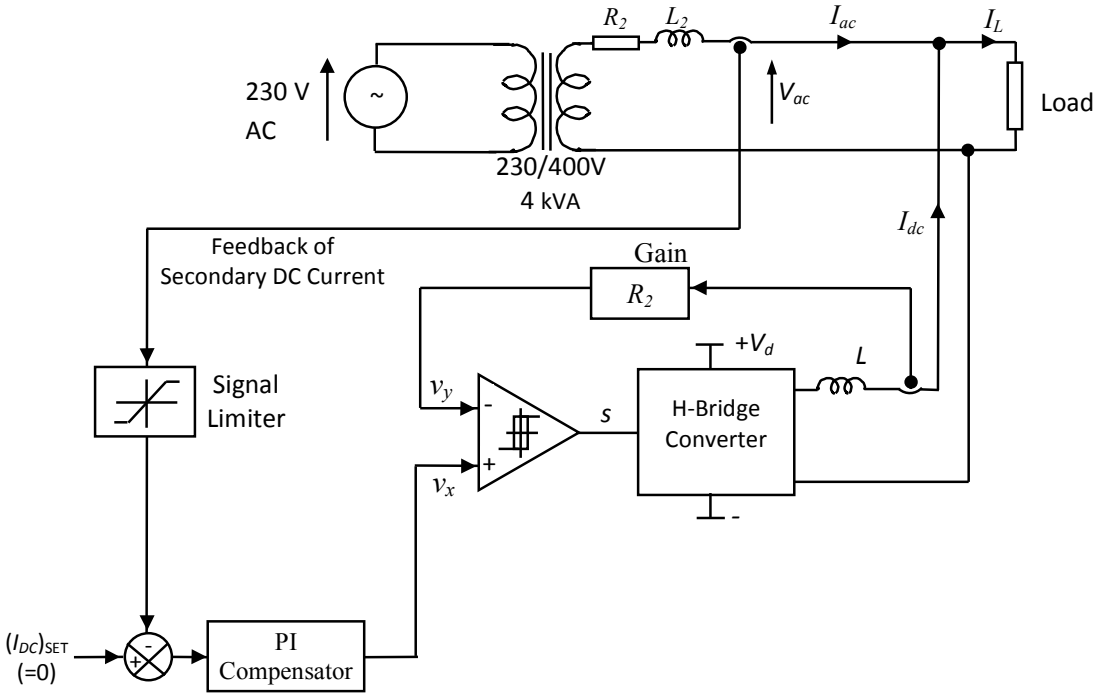

Figure 5.15: Details of Feedback current controller

Closed loop compensator is a crucial unit in the entire DC current elimination strategy where the DC current flowing in the transformer secondary is held zero irrespective of DC current returned by the load. Main functions to be served by the compensator are:

(i) To guarantee zero steady-state DC current in the transformer secondary.

(ii) To settle transient DC current fast in the transformer secondary.

(iii) To restrict peak-overshoot of transient DC current within range in the transformer secondary

Obviously, the set-input to the closed-loop current controller is then zero, as indicated in Figure 5.15. Feedback-signal out from the current sensor contains a disturbance in the form of a transient, caused by the secondary AC voltage component (please refer to section 5.2.2), which need not be passed on to the closed loop compensator. Therefore, a signal limiter was placed on the output of the current sensor to clip out the disturbance component. The limiter was set at $\pm$ 3V which was found adequate to stop the disturbance without significantly affecting the speed of response. This particular setting of the signal-limiter allowed $\pm$12 A span of input DC current for the sensor, which was more than enough for the application in hand.

The decision on the structure of closed loop compensator was taken considering the intended functions and also the action of signal limiter. An integral compensator alone was found adequate to achieve the target. (A parallel proportional control action was considered unnecessary as it tends to produce an initial inrush-current in injected current, which was undesirable)

As long as there is a net DC current in the transformer secondary the DC current sensor output has a non-zero, and accordingly integral compensator output keeps rising. The power electronic converter which converts compensator output to DC current, thus, keeps raising the DC current injected in to the transformer. Transformer secondary takes the difference between the injected DC current and the load produced DC current, which becomes zero when the injected DC current matches the

DC current created by the load. At this instant, the current sensor output becomes zero and the integral compensator output stops further increase. Thus, the control action stops, and the secondary DC current continues to remain at zero. Subsequently, if changes occur in the load-produced DC current, the closed loop controller will act and respond appropriately to bring the DC current in the transformer secondary back to zero.

5.4.1 Transfer Function Model of Feedback Controller

Figure 5.16 shows the transfer function block-diagram of the closed loop current control system. The models of the current-sensor and the power electronic converter are those established in sections 5.2.1 and 5.3.2, respectively. Signal limiter on the current-sensor output is set at $\pm$3V, as described in section 5.4. Feedback gain for output current from the power electronic converter is 0.25, which is the value of the secondary side resistance of the transformer.

AC voltage present at the transformer secondary acts as a disturbance input to the current sensor (see section 5.2.2) and it is modelled accordingly. This is a 50 Hz, 400 V (rms) disturbance input.

$$\left[\left(\sqrt{2}V_{rms}\sin\omega\, t\right) = \frac{\sqrt{2}V_{rms}\omega}{s^2+\omega^2} = \left(\frac{\sqrt{2}\omega s}{s^2+\omega^2}\right)\frac{V_{rms}}{s} == D(s)\frac{V_{rms}}{s} \right. \qquad [5.17]$$

$$D(s) = \left(\frac{\sqrt{2}\omega s}{s^2+\omega^2}\right) = \left(\frac{444.29s}{s^2+98696}\right) \qquad [5.18]$$

According to equation 5.17 and 5.18, the disturbance input can be modelled as a step disturbance of magnitude V_{rms}, followed by transfer function $D(s)$.

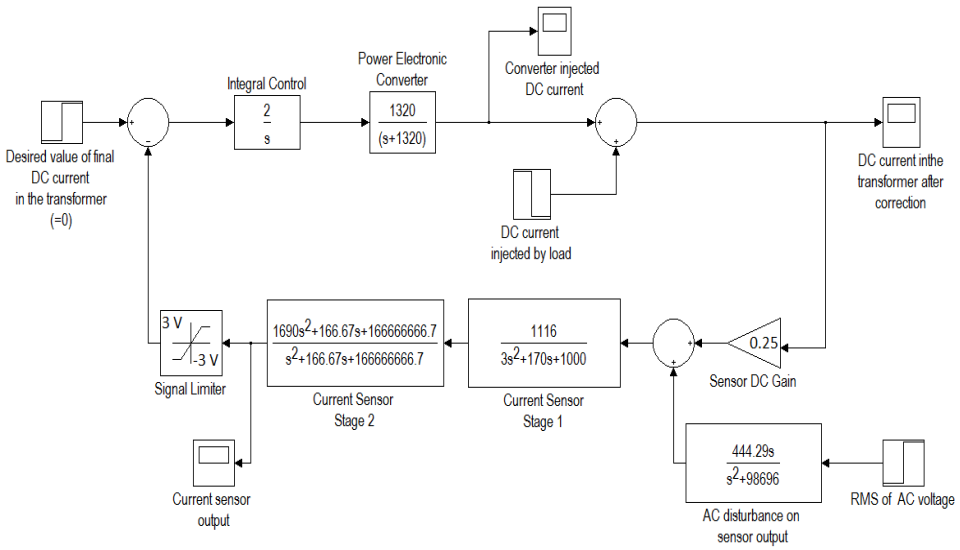

Figure 5.16: Transfer function block diagram of feedback controller

5.4.2 Tuning of closed loop compensator

A value for the integral controller gain K_i was obtained by simulating the closed-loop control system model given in Figure 5.16. A higher value of integral-gain lowered settling-time but raised peak-overshoot of the injected current; opposite happens when integral-gain was lowered. Gain values 1, 2 and 3 all found acceptable (see Table 5.1), and gain of 2 was selected. Corresponding settling time is about 3.0 second and response peak is 2.5A.

Table 5.1: Converter output current parameters for different integral gain values

Integral constant (K_i)	1	2	3
Settling time (S)	4.5	3.0	2.25
Peak response (A)	1.5	2.5	3.7

The complete system of DC current elimination is an intrinsic development from the conceptualization to the detailed final design. Mathematical models derived for individual stages of the system add some versatility to the design. Overall transfer function block diagram of the system is a functional description of the system, and also the basis of the closed loop controller design. Simulations proved the validity of the design in meeting the specifications.

CHAPTER 6

OVERALL PERFORMANCE OF THE CURRENT ELIMINATION SYSTEM

Overall performance of the complete current elimination system was investigated by simulating the final system in MATLAB for different levels of DC current created by loads. Figure 6.1 shows the MATLAB simulation model of the final system.

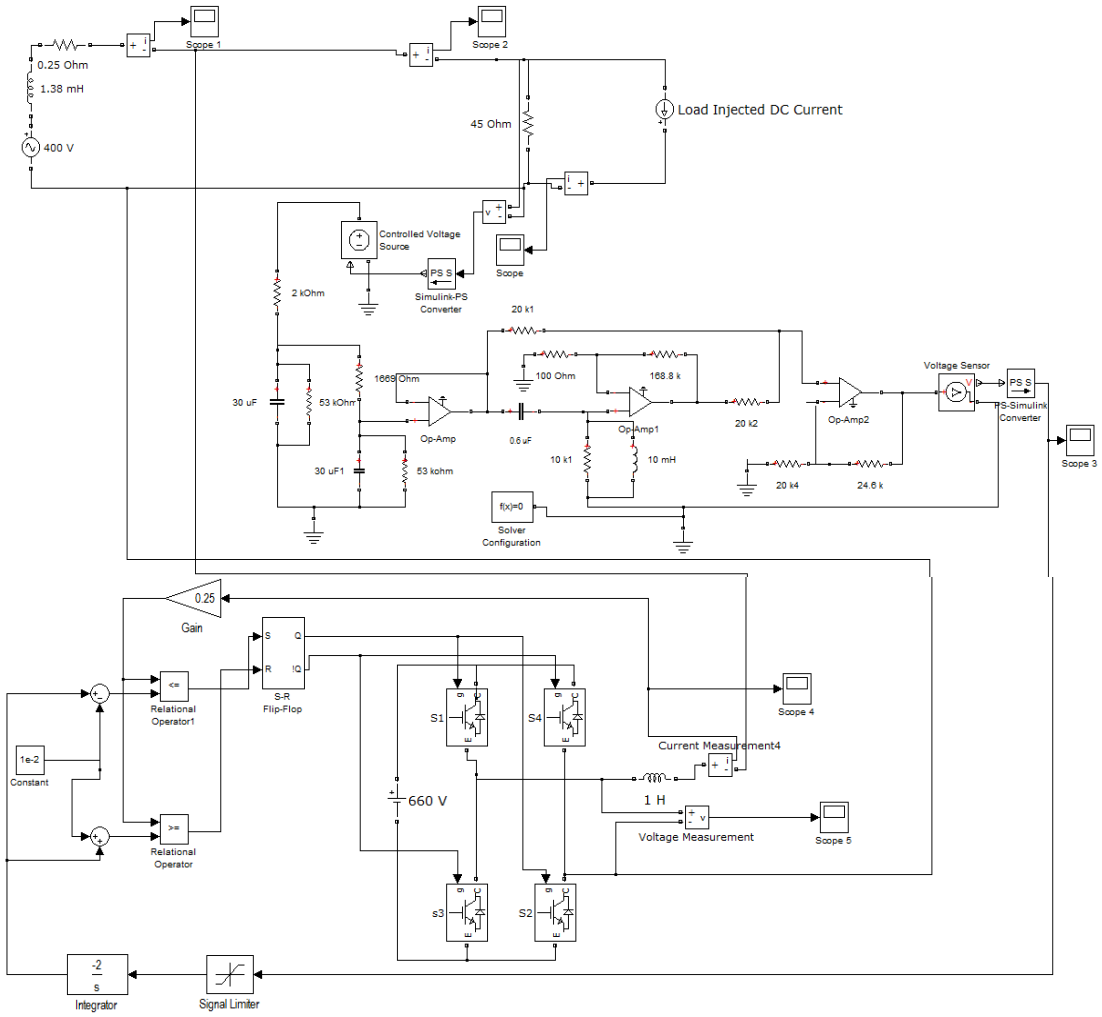

Figure 6.1: MATLAB simulation model for the complete system

The following representative cases were investigated by simulation, and in each case the elimination of DC current component from the transformer secondary was found perfect.

- 40% DC current in load produced by half wave rectification of load current
- 10% DC current in load on top of 80% load, produced by half wave rectification of part of the load current
- 1 A DC current in load on top of 90% load, produced by ideal DC current source
- -1 A DC current in load on top of 90% load, produced by ideal DC current source

6.1 Case of 40% DC current in secondary produced by half wave rectification of load current

Figure 6.1 shows the schematic of the system that was simulated. A series combination of 45Ω resistive load and a diode on the transformer secondary creates a DC current, approximately 40% of rated rms current of the secondary (which is 10 A rms).

$$(I_L)_{DC} = \frac{(I_L)_{pk}}{\pi} = \frac{400\sqrt{2}}{\pi \times 45} = 4.0 \text{ A} \equiv 40\%$$

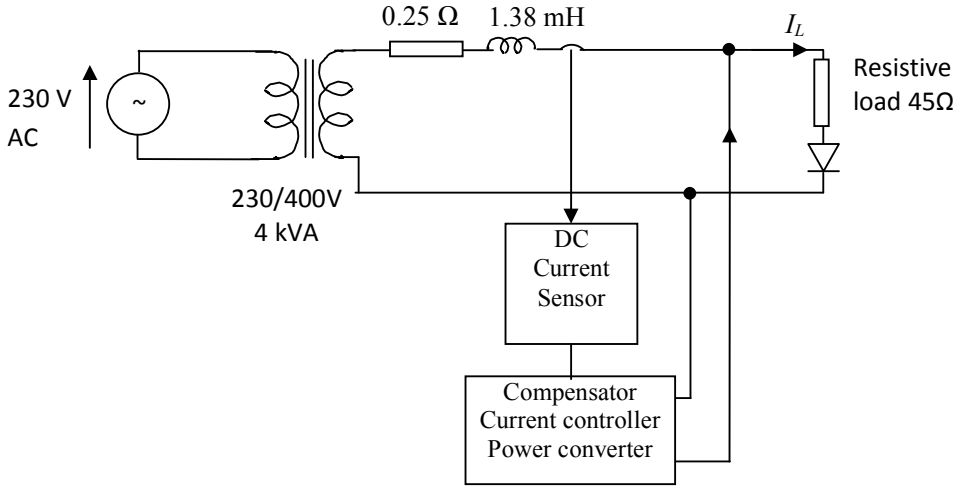

Figure 6.2: System schematic for 40% DC current in in the load produced by half wave rectification of load current

Figure 6.3 shows the current waveform in the load, which is the half-wave rectified current waveform with a mean value equal to 4 A. Figure 6.4 shows the output of the DC current sensor (same as the DC current circulating in the transformer secondary) which, due to the action of the DC current eliminating system has come to zero after a brief transient less than 2 seconds. Figure 6.5 shows the DC current injected to the load by the power electronic converter which is settled at 4 A after the brief transient. It is important to note here that the transient observed in the current sensor output and the DC injection, both, are due to the initial presence of the AC voltage at the sensor input but no similar effects would observe for any subsequent changes to the DC component of load current. Figure 6.6 shows the final current in the transformer secondary, which is the rectified current waveform but without the DC component of 4A.

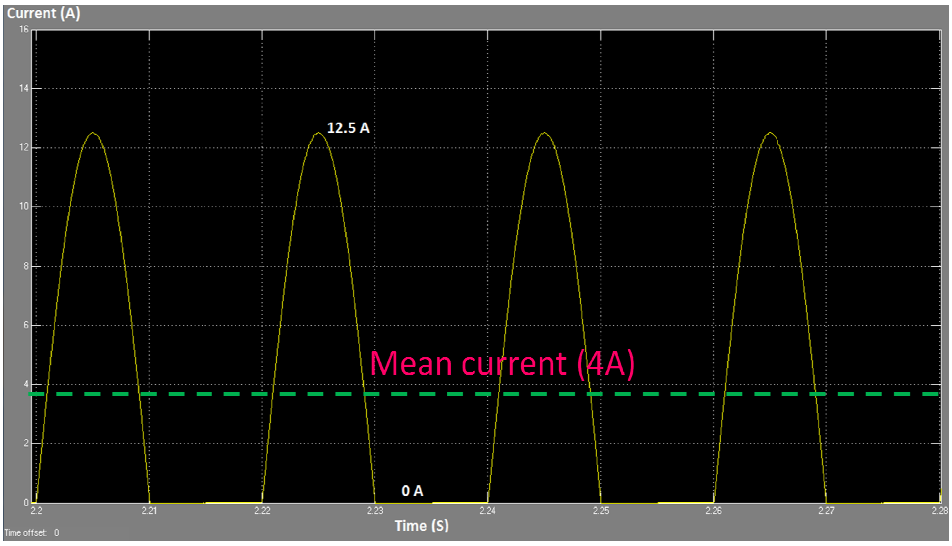

Figure 6.3: Half-wave rectified load current waveform

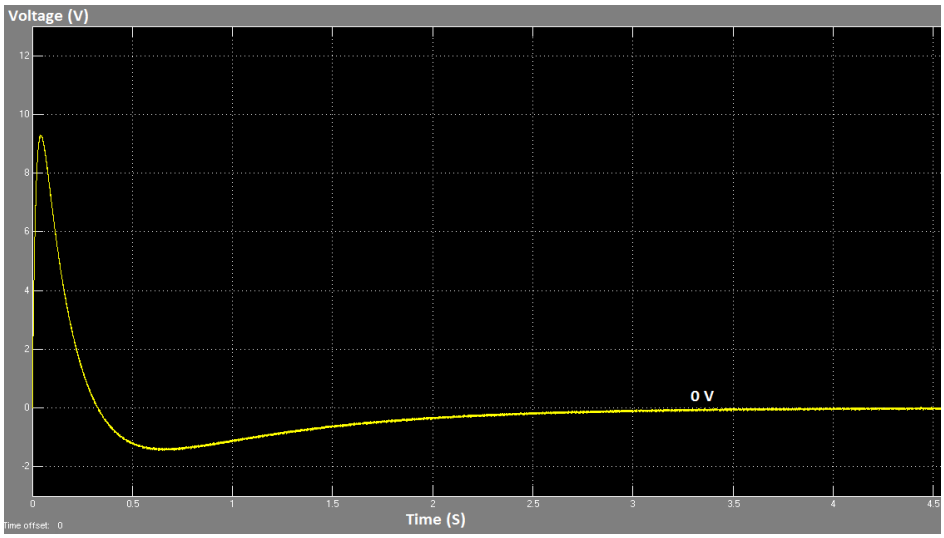

Figure 6.4: Output of the DC current sensor

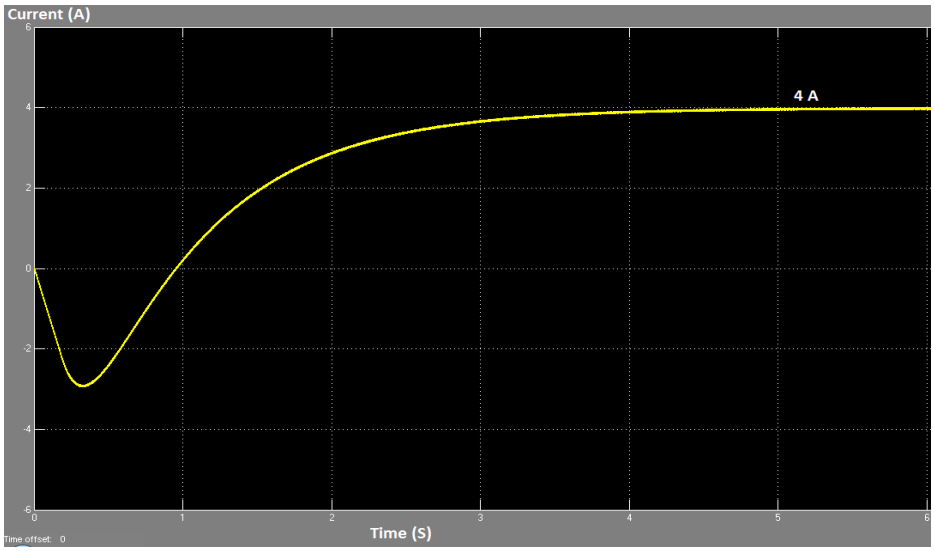

Figure 6.5: DC current injected to the load by the power electronic converter

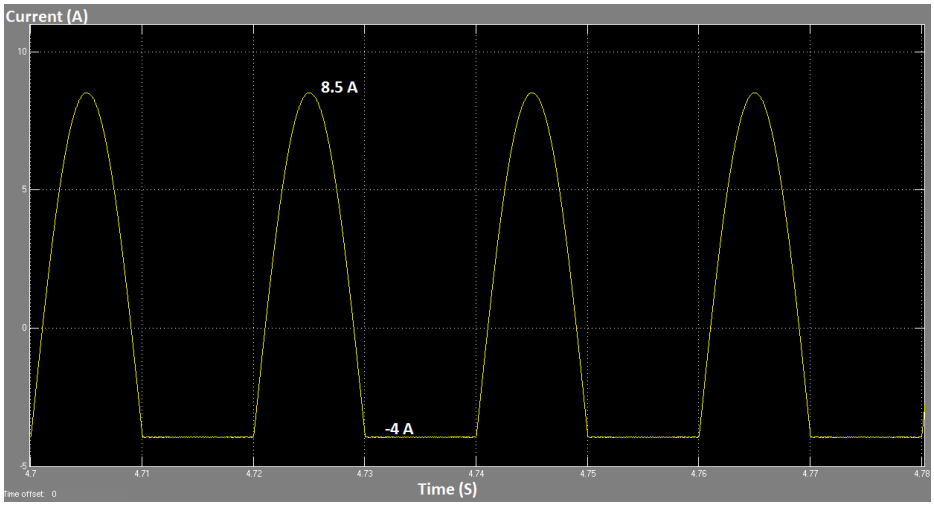

Figure 6.6: Final current in the transformer secondary

It can be observed that the waveform in Figure 6.6 is same as that in Figure 6.3 but now shifted down by 4 A.

6.2 Case of 10% DC current (on top of 80% AC current) in the load, produced by half-wave rectification of part of the load current

Figure 6.7 shows the schematic of the system that was simulated. A series combination of 170Ω resistive load and a diode on the transformer secondary creates a DC current, approximately 10% of rated rms current of the secondary (which is 10 A rms). The 58 Ω resistive load creates the AC component of load current.

$$(I_L)_{DC} = \frac{400\sqrt{2}}{\pi \times 170} = 1.0 \text{ A} \equiv 10\%$$

$$(I_L)_{AC} = \left(\frac{400}{58}\right) + \frac{1}{2}\left(\frac{400}{170}\right) = 8.0 \text{ A} \equiv 80\%$$

(RMS value of the fundamental component of current in the diode branch is equal to 50% of the rms current without the diode, i.e diode shorted).

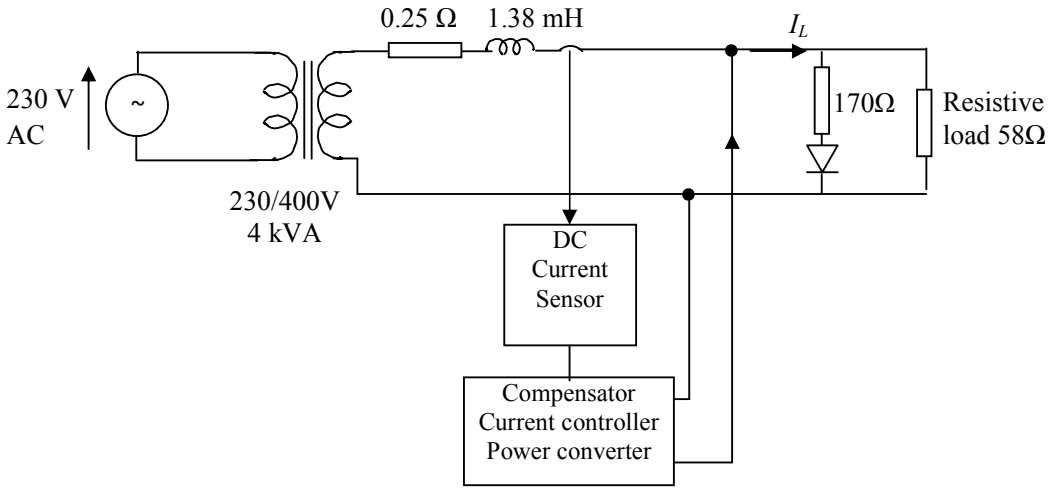

Figure 6.7: System schematic for 10% DC current (on top of 80% AC current) in the load produced by half wave rectification of part of the load current

Figure 6.8 shows the current waveform in the load, which has a 13 A positive peak and -9.7 A negative peak, with a mean value of 1 A. Figure 6.9 shows the output of the DC current sensor (i.e. DC current circulating in the transformer secondary) which, due to the action of the DC current eliminating system has come to zero after a brief transient lasting about 1 second. Figure 6.10 shows the DC current injected to the load by the power electronic converter which is settled at 1 A after the brief transient. Figure 6.11 shows the final current in the transformer secondary, which is the load current waveform without the DC component of 1A.

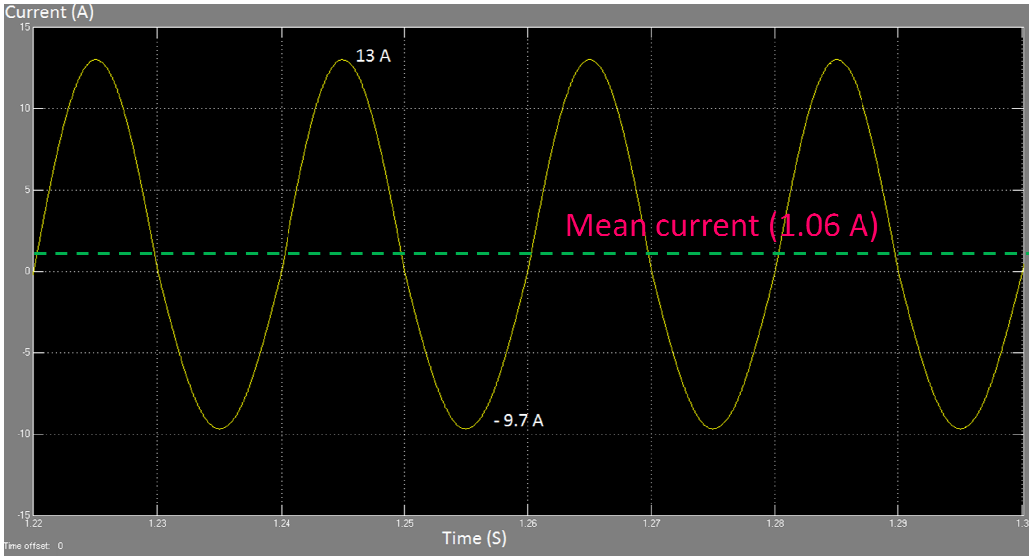

Figure 6.8: Load current waveform with 10% DC on top of 80% AC

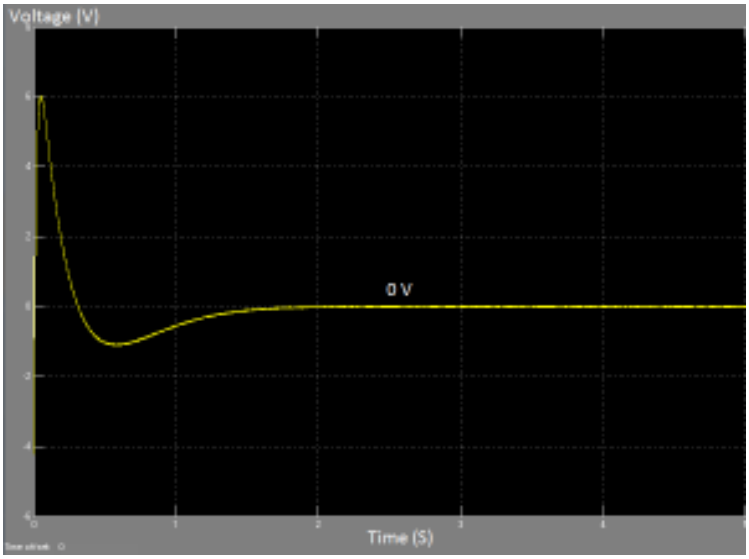

Figure 6.9: Output of DC current sensor

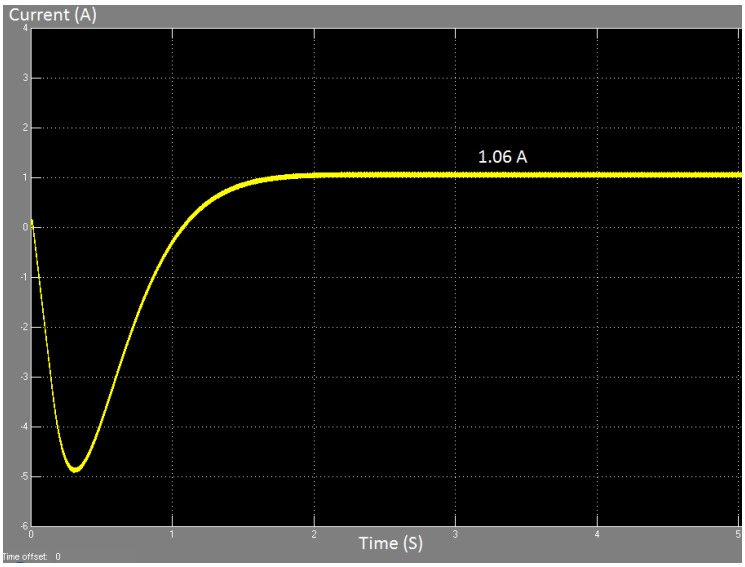

Figure 6.10: DC current injected to the load by the power electronic converter

.

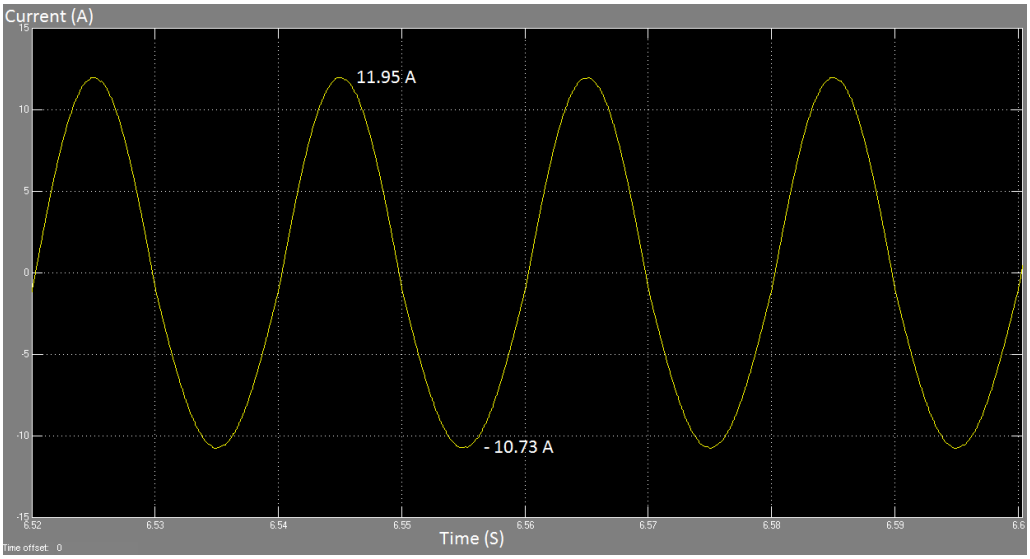

Figure 6.11: Final current in the transformer secondary

It can be observed that the current waveform in Figure 6.11 is same as that in figure 6.8 but now shifted down by 1 A.

6.3 Case of 1 A DC current (on top of 90% AC current) in the load produced by an ideal DC source at the load

Figure 6.12 shows the schematic of the system that was simulated. The 45 Ω resistive load established 90% load current, and the ideal DC current source introduced 1 A DC current in to the load.

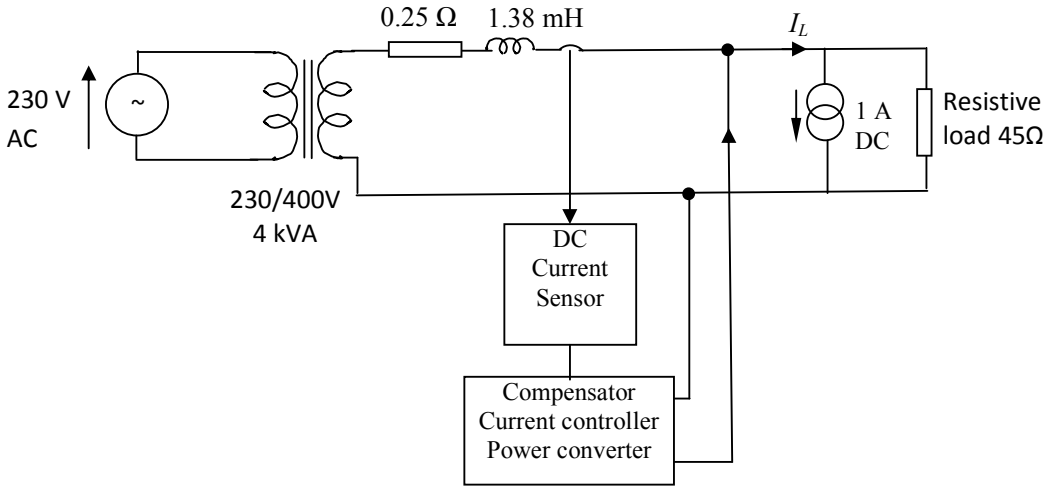

Figure 6.12: System schematic for 1A DC current (on top of 90% AC current) in the load produced by an ideal current source

Figure 6.13 shows the current waveform in the load, which has a 13.4 A positive peak and -11.4 A negative peak, with a mean value of 1 A. Figure 6.14 shows the output of the DC current sensor (i.e. DC current circulating in the transformer secondary) which, due to the action of the DC current eliminating system has come to zero after a brief transient less than 0.5 second. Figure 6.15 shows the DC current injected to the load by the power electronic converter which is settled at 1 A after the brief transient. Figure 6.16 shows the final current in the transformer secondary, which is the load current waveform without the DC component of 1A.

In Figure 6.14, it is observed that, initially, the output of the DC current sensor exhibits a -45 V step jump of. This is the initial -45V built across the transformer secondary that the sensor has detected, created by the 1 A step current through the 45Ω load resistance. Initially, 1 A step current goes entirely through the 45 Ω load resistance as the leakage inductance in the transformer secondary looks like an open circuit for the step change.

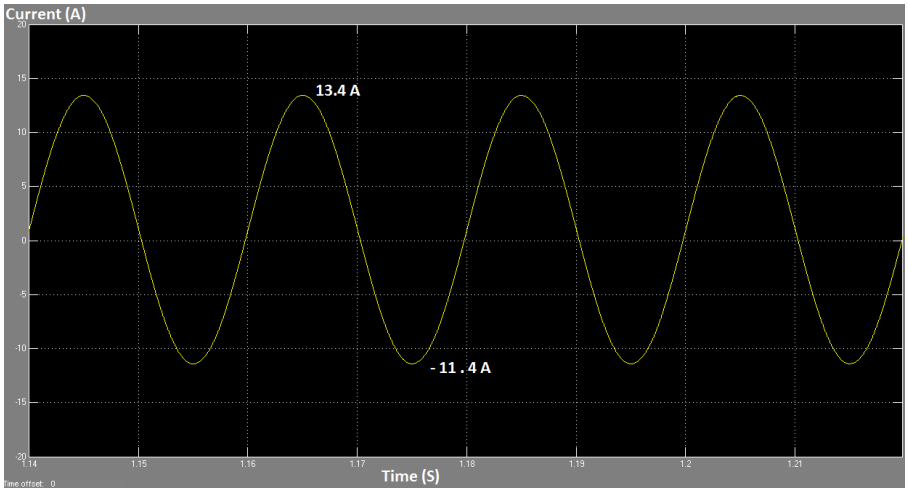

Figure 6.13: Load current waveform with 1A DC on top of 90% AC current

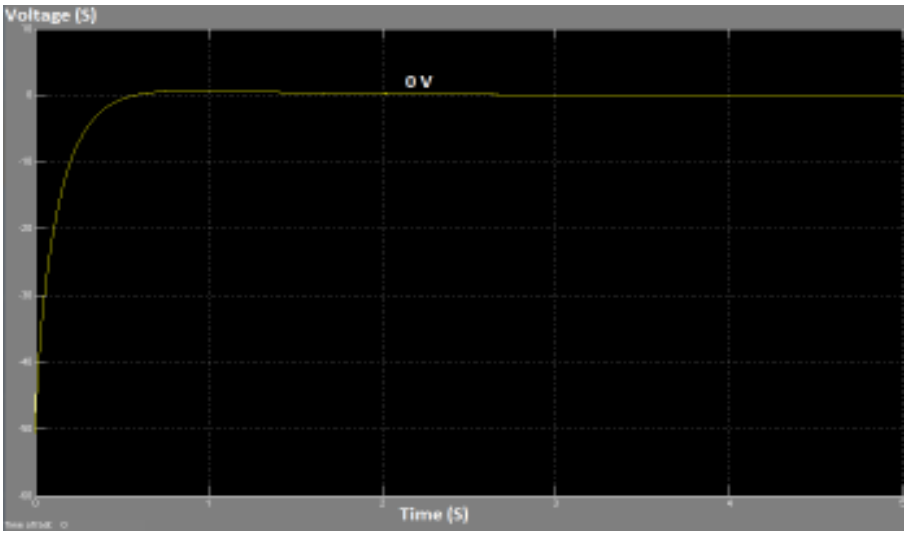

Figure 6.14: Output of DC current sensor

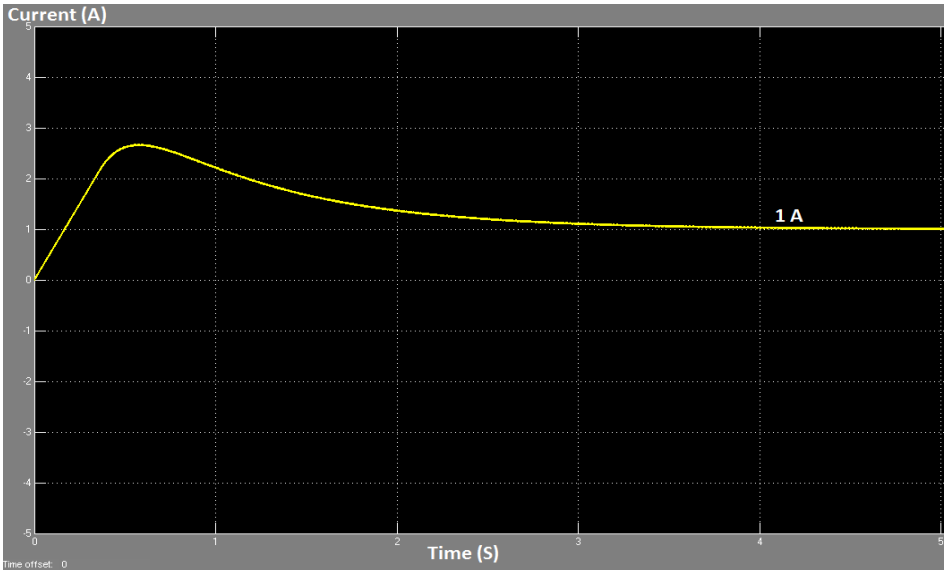

Figure 6.15: DC current injected to the load by the power electronic converter

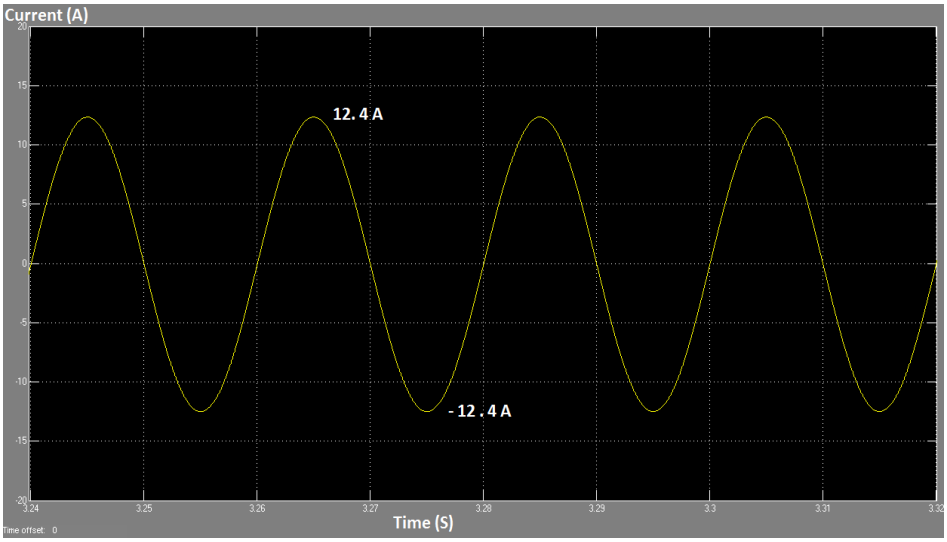

Figure 6.16: Final current in the transformer secondary

It can be observed that the final transformer current is now the 90% resistive load current (with equal positive and negative half-cycles) without the 1A DC component.

6.4 Case of -1 A DC current (on top of 90% AC current) in the load produced by an ideal DC source at the load

Figure 6.17 shows the schematic of the system that was simulated. The 45 Ω resistive load established 90% load current, and the ideal DC current source introduced -1 A DC current in to the load (notice that the 1A DC current source is now connected in reverse direction compared to the same in Figure 6.12, implying a returning DC current towards the transformer secondary).

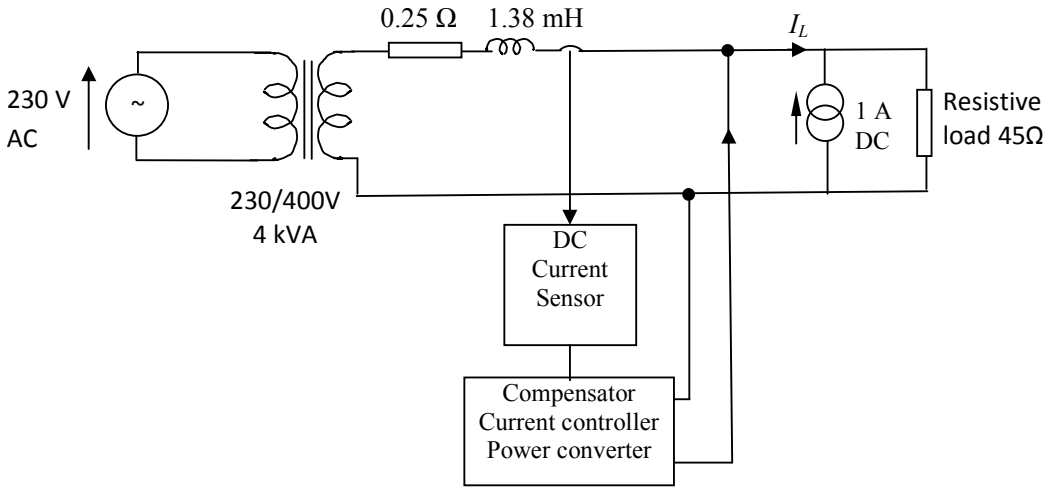

Figure 6.17: System schematic for -1A DC current (on top of 90% AC current) in the load produced by an ideal current source

Figure 6.18 shows the current waveform in the load, which has an 11.5 A positive peak and -13.5 A negative peak, with a mean value of -1 A. Figure 6.19 shows the output of the DC current sensor (i.e. DC current circulating in the transformer secondary) which, due to the action of the DC current eliminating system has come to zero after a brief transient less than 0.5 second. Figure 6.20 shows the DC current injected to the load by the power electronic converter which is settled at -1 A after the brief transient. Figure 6.21 shows the final current in the transformer secondary, which is the load current waveform without the DC component of -1A.

In Figure 6.19, it is observed that, initially, the output of the DC current sensor exhibits a 45 V step jump of. This is the initial 45V built across the transformer secondary that the sensor has detected, created by the 1 A step current through the 45Ω load resistance. Initially, 1 A step current goes entirely through the 45 Ω load resistance as the leakage inductance in the transformer secondary looks like an open circuit for the step change.

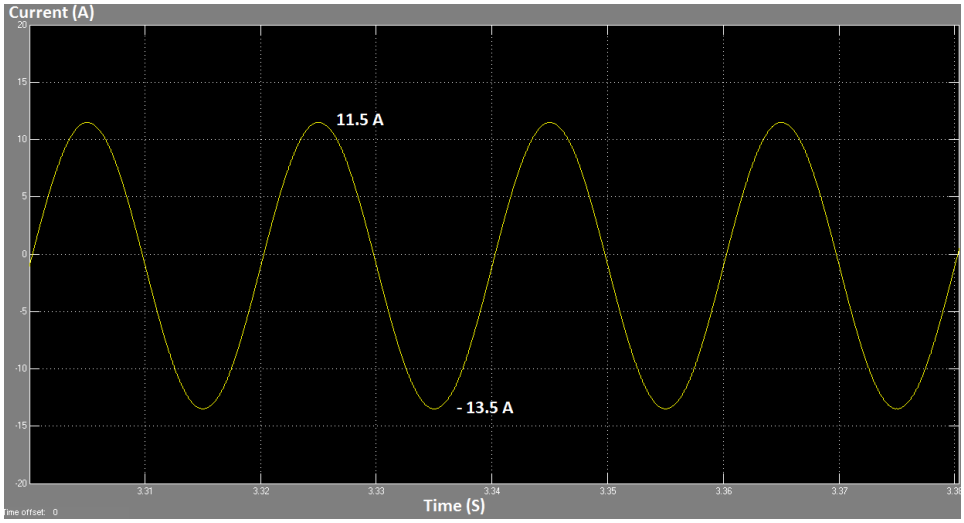

Figure 6.18: Load current waveform with -1A DC on top of 90% AC current

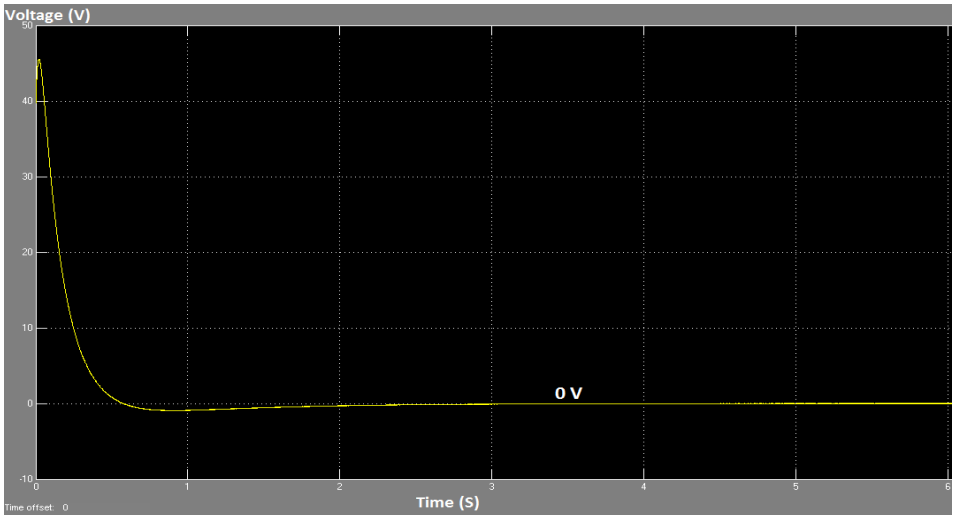

Figure 6.19: Output of DC current sensor

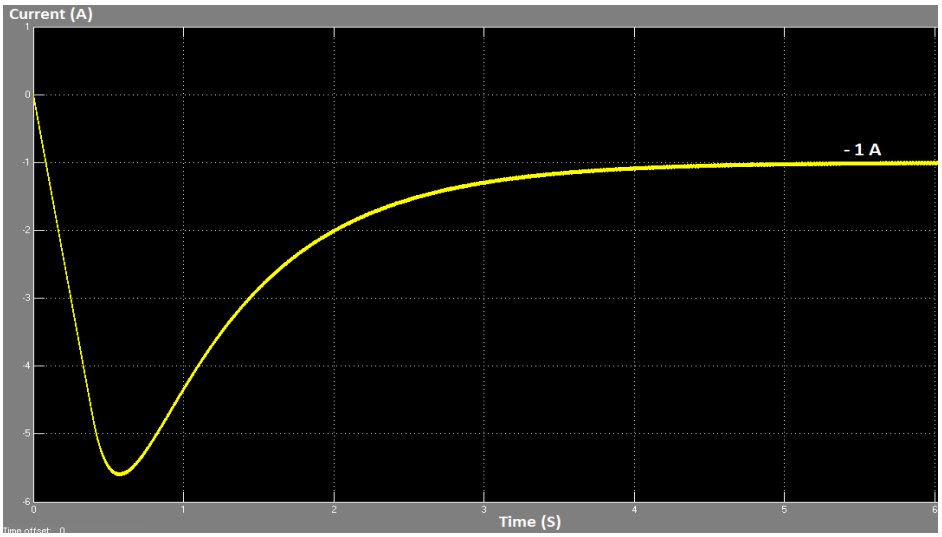

Figure 6.20: DC current injected to the load by the power electronic converter

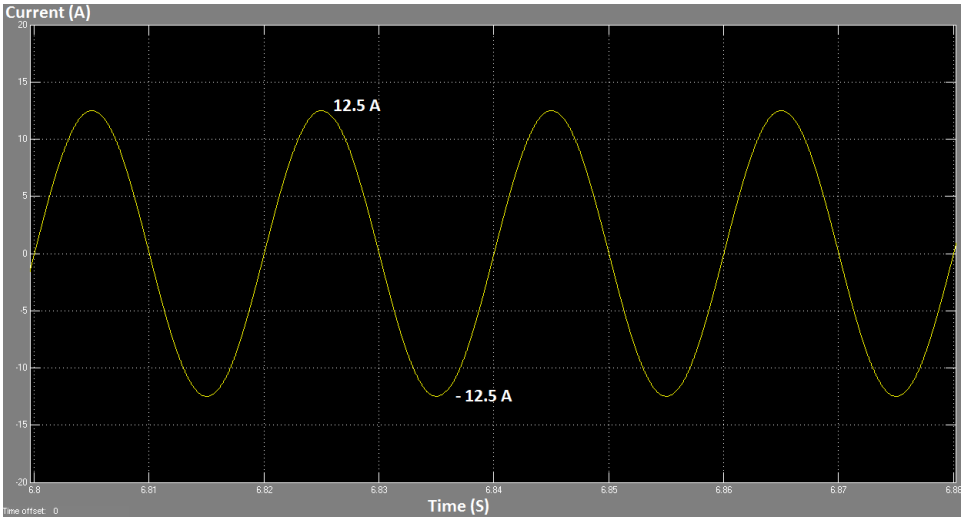

Figure 6.21: Final current in the transformer secondary

It can be observed that the final current in the transformer secondary is now the 90% resistive load current (with equal positive and negative half-cycles) without the -1A DC component.

In summary, the results of simulation show that the DC current in the transformer secondary has been eliminated completely in all cases of load-injected DC current.

CHAPTER 7

CONCLUSION

This project was about investigating the effects of DC current (created by the loads) on the operation of a transformer, designing a power electronic based system for complete diverting of DC current away from the transformer, simulating the designed system for different levels of DC current to test the effectiveness of the design in meeting the said objectives, and comparing the simulation outcomes with the practically observed results to validate the design.

In this context, first a transformer was subjected to a series of laboratory tests to observe its behavior with intentionally created DC current in the transformer secondary, on top of the normal AC load current. Those observations were then assessed and interpreted with theoretical models on the magnetization-phenomenon in real transformers, which set the stage for broader investigations on various scenarios of DC mixing on top of load current.

When it comes to the simulation of transformers with due focus on magnetization aspects, especially shifting of magnetic operating point of iron due to the mix of DC current, the commonly available transformer models in simulation tools were not helpful. So, it was necessary to develop our own model for this purpose. Identifying the magnetization characteristic for the particular grade of steel used in the transformer was necessary. Without going down to the material characteristic, it was decided to use the no-load test data, especially no-load current and voltage, as an input to the model which contained the information of magnetization characteristic. The model so developed was used in all simulations and found that the test and simulated responses were matching remarkably. Many different cases of DC current mix ups were simulated and the behavior investigated using the model.

Design of a suitable current sensor that can accurately detect small amounts of DC current flowing in the transformer secondary on top of a large AC current was a real

challenge. Several proposals have been found in the literature, some even patented, but they are either too complicated to implement or not giving the level of accuracy needed. In our design, we used a different approach, a new concept, to implement the sensor relatively easily with best accuracy. Instead of current the voltage across the transformer secondary was sensed, which contained the information of DC current (because DC current is creating a DC voltage component across the winding resistance in the secondary). A dual *RC* voltage-divider stage, followed by a novel active low-pass filter was at the heart of this sensor and its performance was found extremely satisfactory.

The DC current elimination system was architected to be implemented on each phase, separately, as the DC current on individual phases vary independently. Therefore, a simple H-bridge configured power circuit was selected and it was controlled to deliver the desired DC current through hysteresis current control in closed loop. The DC voltage input to the H-bridge was provided separately, but deliverable from the AC supply. Closed loop control was implemented with an integral controller, instead of typical proportional plus integral controller, mainly due to the use of a signal limiter on the output of the current sensor with which a proportional gain was found not desirable to achieve the desired response. The signal limiter on the current sensor output was a necessity to arrest the transient peak created by AC voltage present at the sensor input.

Simulation of the complete current elimination system was done in MATLAB software, and it was proved that the system can divert any DC current returned or demanded by the load away from the secondary of the transformer. DC current created by half-wave rectifiers as well as ideal step DC current sources at the load could be diverted effectively away from the transformer, for both polarities.

Some of the highlights or concluding remarks are:

- Model of transformer that uses no-load test data to derive magnetization characteristic is sufficiently accurate to imitate the true behavior of the transformer under the influence of DC current created by loads.

- DC current circulating through the secondary of a transformer creates asymmetric magnetization leading to creation of even higher DC current level at the input side, beside its other effects in the transformer itself.

- A novel current-sensor was developed for detecting small DC current superimposed with large AC current and its performance was extremely satisfactory.

- A DC current injection system was developed and it can completely divert the DC current (returned or demanded by loads) away from the transformer.

- H-bridge power circuit with hysteresis current control was sufficient to deliver DC current within ±0.01A tolerance with moderate switching frequency in the range 4.5 kHz and 15 kHz inside the current injection system.

Continuation of this study for three-phase transformers for different core/winding combinations and actual hardware implementation of the current elimination system remain yet to be done as future work.

REFERENCE LIST

[1] University of Strathclyde, "DC injection into low voltage AC networks", DTI Commissioned Report, June 2005.

[2] A.Ahfock, and L.Bowtell, "Direct current offset controller for transformerless single phase photovoltaic grid-connected inverters", IET Renewable Power Generation, Vol. 4, 2010, Iss.5, pp.428-437.

[3] D.J.Atkinson, W.M.Blewitt, J.Kelly and R.A.Lakin, "Approach to low cost prevention of DC injection in transformerless grid connected inverters" , IET Power Electronics, Vol. 3, 2010, Iss.1, pp. 111-119.

[4] T.Ahfock, and L.Bowtell, "DC offset elimination in a single phase grid-connected photovoltaic system", Faculty of Engineering and Surveying, University of Southern Queensland, Australia.

[5] M.Armstrong, D.J.Atkinson, C.M.Johnson and T.D.Abeyasekera, "Auto calibrating DC link current technique for transformerless grid connected H-bridge inverter systems", IEEE Transactions on Power Delivery, Vol. 21, No. 5, September 2006.

[6] V.Salas, E.Olias, M.Alonso, F.Chenlo and A.Barrado, "DC current injection into the network from PV grid inverters", IEEE Transaction on Power Delivery, 2006.

[7] H.Haeberlin, "Evolution of inverters for grid connected systems from 1989 to 2000", 17th European Photovoltaic Solar Energy Conference, October 2001.

[8] A.K. Ziemer, "The effect of DC current on power transformers", University of Southern Queensland, Australia.

[9] R.Sharma, "Removal of DC offset current from transformerless PV inverters connected to utility", Proceedings of the 40th International Universities Power Engineering Conference, Cork Institute of Technology, Ireland, pp.1230-1234.

[10] L. Buticchi, G. Franceschini, and E. Lorenzani, "A DC offset current compensation strategy in transformerless grid conneted power converters", IEEE Transactions on Power Delivery, Vol. 26, No. 4, October 2011.

[11] Fronius International, "High frequency transformer with transformer switchover", https://www.fronius.com/cps/rde/xbcr/SID-4725BB5C-2C0F62DA/fronius_international/SE_TA_High_Frequency_Transformer_With_Transformer_Switchover_EN_320487_snapshot.pdf

APPENDICE A: MATLAB CODES

Table A.1: MATLAB code for simulation of input current on open circuit

```
clc;
Is(1) =0;
Y (1) = 0;
Delt = 0.0000001;
R = 0.083;
L=0.000458;
Rc=1322.5;
t=0;

for k= 1:1:200000
Vs(k) = 340*cos(314.15*t);

I1(k)= (-0.4746* Y(k)^6)+(2.0944* Y(k)^5)+(0.7191* Y(k)^4)-
       (0.6226* Y(k)^3)-(0.2973* Y(k)^2)+(0.0999* Y(k))- 0.014;

Is(k+1) = Is(k)*(1-(Delt*(R+Rc)/L)) + (Delt*Vs(k)/L)
          +(Delt*Rc*I1(k)/L);

Y (k+1) = Y (k) + Delt*Rc*(Is(k)-I1(k));

t = t + Delt;
end

plot(Is);
grid on;
xlswrite('Test.xlsx',Is');
```

Table A.2: MATLAB code for simulation of input current with load on secondary

```
clc;
Is(1) = 0;
I2(1)= 0;
Y(1) = 0;
Delt = 0.0000001;
R1 = 0.083;
R2 = 0.083;
L1=0.000458;
L2=0.000458;
RL= 45;
Rc=1322.5;
t=0;

 for k= 1:1:400000
 Vs(k) = 340*cos(314.15*t);

 I1(k)= (-0.4746* Y(k)^6)+(2.0944* Y(k)^5)+(0.7191* Y(k)^4)-
           (0.6226*  Y(k)^3)-(0.2973* Y(k)^2)+(0.0999* Y(k))-0.014 +
           (40/23)*I2(k);

 Is(k+1) = Is(k)*(1-(Delt*(R1+Rc)/L1)) + (Delt*Vs(k)/L1)
              +(Delt*Rc*I1(k)/L1);

 I2(k+1) = I2(k)*(1-(Delt*(R2+RL)/L2)) + (Delt*(40/23)*Rc*(Is(k)-
              I1(k))/L2);

 Y(k+1) = Y(k) + Delt*Rc*(Is(k)-I1(k));

    t = t + Delt;

end

 plot(Is);
 grid on;
 xlswrite('Test22_Is.xlsx',Is');
 xlswrite('Test22_I2.xlsx',I2');
 xlswrite('Test22_Flux.xlsx', Y ');
```

Table A.3: MATLAB code for simulation of input current with heavy DC current injected to the secondary

```
clc;
Is(1) = 0;
I2(1)= 0;
Y(1) = -1.29;
Delt = 0.0000001;
R1 = 0.083;
R2 = 0.083;
L1=0.000458;
L2=0.000458;
RL= 45;
Rc=1322.5;
t=0;
for k= 1:1:800000
 Vs(k) = 340*cos(314.15*t);

 I1(k)= (-0.4746* Y(k)^6)+(2.0944* Y(k)^5)+(0.7191* Y(k)^4)-
       (0.6226* Y(k)^3)-(0.2973* Y(k)^2)+(0.0999* Y(k))-0.014 +
        (40/23)*I2(k);

 Is(k+1) = Is(k)*(1-(Delt*(R1+Rc)/L1)) +(Delt*Vs(k)/L1)
           +(Delt*Rc*I1(k)/L1);

 I2(k+1) = I2(k)*(1-(Delt*(R2+RL)/L2)) + (Delt*(40/23)*Rc*(Is(k)-
          I1(k))/L2);

If (I2(k+1)<= 0)
   I2(k+1) = 0;
end

  Y(k+1) = Y(k) + Delt*Rc*(Is(k)-I1(k));

  t = t + Delt;
 end

 plot(Is);
 grid on;
 xlswrite('Test7.xlsx',Is');
 xlswrite('Test8.xlsx',I2');
 xlswrite('Test9.xlsx', Y ');
```

Table A.4: MATLAB code for simulation of input current with small DC current injected to the secondary

```
clc;
Is(1) = 0;
I2(1)= 0;
Y(1) = 1.04;
I3(1)= 0;
Delt = 0.0000001;
R1 = 0.083;
R2 = 0.083;
L1=0.000458;
L2=0.000458;
RL1= 58;
RL2= 170;
Rc=1322.5;
t=0;

 for k= 1:1:800000
 Vs(k) = 340*cos(314.15*t);

 I1(k)= (-0.4746* Y(k)^6)+(2.0944* Y(k)^5)+(0.7191* Y(k)^4)-
        (0.6226* Y(k)^3)-   (0.2973* Y(k)^2)+(0.0999* Y(k))-0.014 +
       (40/23)*I2(k);

 Is(k+1) = Is(k)*(1-(Delt*(R1+Rc)/L1)) + (Delt*Vs(k)/L1)
           +(Delt*Rc*I1(k)/L1);

 I2(k+1) = I2(k)*(1-(Delt*(R2+RL1)/L2)) + (Delt*(40/23)*Rc*(Is(k)-
           I1(k))/L2)+ (Delt*RL1*I3(k)/L2);

 I3(k+1) = I2(k+1)*RL1/(RL2+RL1);

    If (I3(k+1)>= 0)
        I3(k+1) = 0;
    end
Y(k+1) = Y(k) + Delt*Rc*(Is(k)-I1(k));
t = t + Delt;
end
plot(Is);
grid on;
xlswrite('Test20_Is.xlsx',Is');
xlswrite('Test20_I2.xlsx',I2');
xlswrite('Test20_I3.xlsx',I3');
xlswrite('Test20_Flux.xlsx', Y');
xlswrite('Test14.xlsx',Vs');
```